

Adjoint QCD on $\mathbb{R}^3 \times S^1$ with twisted fermionic boundary conditions

Tatsuhiro Misumi^a and Takuya Kanazawa^b

^a*Department of Physics, and Research and Education Center for Natural Sciences, Keio University, Hiyoshi 4-1-1, Yokohama, Kanagawa 223-8521, Japan*

^b*iTHES Research Group and Quantum Hadron Physics Laboratory, RIKEN, Wako, Saitama 351-0198, Japan*

E-mail: misumi@phys-h.keio.ac.jp, takuya.kanazawa@riken.jp

ABSTRACT: We investigate QCD with adjoint Dirac fermions on $\mathbb{R}^3 \times S^1$ with generic boundary conditions for fermions along S^1 . By means of perturbation theory, semiclassical methods and a chiral effective model, we elucidate a rich phase structure in the space spanned by the S^1 compactification scale L , twisted fermionic boundary condition ϕ and the fermion mass m . We found various phases with or without chiral and center symmetry breaking, separated by first- and second-order phase transitions, which in specific limits ($\phi = 0$, $\phi = \pi$, $L \rightarrow 0$ and $m \rightarrow \infty$) reproduce known results in the literature. In the center-symmetric phase at small L , we show that Ünsal's bion-induced confinement mechanism is at work but is substantially weakened at $\phi \neq 0$ by a linear potential between monopoles. Through an analytic and numerical study of the PNJL model, we show that the order parameters for center and chiral symmetries (i.e., Polyakov loop and chiral condensate) are strongly intertwined at $\phi \neq 0$. Due to this correlation, a deconfined phase can intervene between a weak-coupling center-symmetric phase at small L and a strong-coupling one at large L . Whether this happens or not depends on the ratio of the dynamical fermion mass to the energy scale of the Yang-Mills theory. Implication of this possibility for resurgence in gauge theories is briefly discussed. In an appendix, we study the index of the adjoint Dirac operator on $\mathbb{R}^3 \times S^1$ with twisted boundary conditions, which is important for semiclassical analysis of monopoles.

Contents

1	Introduction	1
2	Center symmetry realization	5
2.1	Phase structure at small S^1	5
2.1.1	One-loop effective potential	6
2.1.2	Phase diagram for $(N_c, N_f^D) = (2, 1), (3, 1)$ and $(3, 2)$	7
2.1.3	Mass gap and confinement from semiclassics	10
2.2	Phenomenological gluonic potential	15
3	Impact of chiral symmetry breaking	17
3.1	Chiral symmetry in QCD(adj)	18
3.2	PNJL model: an analytical study	20
3.2.1	Trivial holonomy	22
3.2.2	Center-symmetric holonomy	24
3.3	PNJL model: numerical results	26
4	Summary and discussion	30
A	Index theorem with twisted boundary conditions	32
B	A remark on the literature	34

1 Introduction

Compared to QCD with quarks in the fundamental representation of the gauge group, $SU(N)$ gauge theories with adjoint fermions [QCD(adj)] have many distinctive features that make QCD(adj) an important area of research. Firstly, adjoint fermions do not break the center symmetry \mathbb{Z}_N and there is a well-defined deconfinement transition in QCD(adj). In lattice simulations the deconfinement transition was found to occur at a much lower temperature than the chiral phase transition [1–4]. This is in contradistinction to QCD with fundamental quarks, where the two transitions (crossovers) occur at around the same temperature. Understanding the origin of such discrepancy may bring us new insights into the mechanism of confinement and chiral symmetry breaking in QCD and QCD(adj).

Secondly, QCD(adj) is free from the notorious sign problem even at nonzero chemical potential and can be simulated with standard lattice QCD methods [5–7]. This peculiar feature originates from a special anti-unitary symmetry of the Dirac operator in the adjoint representation. Owing to this symmetry, the pattern of chiral symmetry breaking is not the standard one $SU(N_f^D)_R \times SU(N_f^D)_L \rightarrow SU(N_f^D)_V$, but rather $SU(N_f^W) \rightarrow SO(N_f^W)$ [8], where N_f^D is the number of Dirac fermions and $N_f^W (= 2N_f^D)$ is that of Weyl fermions. Part

of the Nambu-Goldstone (NG) modes are diquarks, and their Bose-Einstein condensation (BEC) at nonzero chemical potential has been studied in chiral perturbation theory [6, 9, 10] and in chiral effective models [11, 12]. A relativistic analogue of the BEC-BCS crossover from low to high density is also conjectured [13]. These developments in QCD(adj) make it an attractive laboratory for methods and concepts of finite-density QCD.

Thirdly, QCD(adj) with a single Majorana fermion is nothing but the $\mathcal{N} = 1$ supersymmetric Yang-Mills (SYM) theory and its non-perturbative dynamics has been studied for long [14], serving as an archetype of strongly-coupled supersymmetric gauge theories.

Other topics related to QCD(adj) include the large- N volume independence and the large- N orbifold/orientifold equivalences [15] and the walking technicolor scenario [16]. A short review on QCD(adj) is available [17].

Now let us consider QCD(adj) on $\mathbb{R}^3 \times S^1$. As S^1 is not simply connected we need to specify boundary conditions for fields. In this paper we always assume the periodic boundary condition (PBC) for gauge fields. The boundary condition for fermions can be parametrized as

$$\Psi(\vec{x}, x_4 + L) = e^{i\phi} \Psi(\vec{x}, x_4), \quad (1.1)$$

where L is the circumference of S^1 . While $\phi = \pi$ (anti-periodic boundary condition, ABC) corresponds to thermal compactification, other choices are also of physical interest due to several reasons. To name but a few:

- PBC ($\phi = 0$) is useful in supersymmetric gauge theories because it does not break SUSY [18]. In SYM on $\mathbb{R}^3 \times S^1$ with PBC for fermions, various non-perturbative phenomena such as confinement and mass gap generation have been shown analytically with semiclassical methods [19–21].
- Twisted boundary condition (1.1) offers a useful probe to QCD at finite temperature and density. In SU(3) QCD with fundamental fermions, the partition function is periodic in ϕ with a period of $2\pi/3$ (the Roberge-Weiss periodicity) and the dependence of observables on ϕ may distinguish the confined/deconfined phases [22]. It is also suggested that QCD at generic ϕ could help us investigate the phase structure of finite-density QCD, because (1.1) is equivalent to an *imaginary* chemical potential, which causes no sign problem [5]. Such a direction has been actively pursued with lattice simulations [23–28] and chiral effective models [29–31]. The twisted boundary condition is also used to define the so-called dual quark condensate and the dressed Polyakov loop [32–35].
- SU(N) QCD(adj) on $\mathbb{R}^3 \times S^1$ with $\phi = 0$ exhibits gauge symmetry breaking $SU(N) \rightarrow U(1)^{N-1}$ [36]¹, which is verified in lattice simulations [37, 38]. This phenomenon, called Hosotani mechanism, is essential to the idea of gauge-Higgs unification [36, 39–42]. In perturbation theory, the low-energy spectrum after gauge symmetry breaking consists of free massless photons and fermions. However this is not the end of the

¹This was shown by Hosotani for $N_f^W \geq 2$ using a one-loop effective potential [36]. For $N_f^W = 1$, by contrast, the bosonic and fermionic contributions cancel to all orders in perturbation theory owing to supersymmetry and a non-perturbative treatment is required [21].

story: as first pointed out by Ünsal, topological objects (monopole-instantons and their bound states called *bions*) lead to mass gap and confinement in the small- S^1 semiclassical domain [43, 44]. This can be viewed as a 4d generalization of Polyakov’s treatment on the 3d Georgi-Glashow model [45] as well as a non-SUSY generalization of preceding works on semiclassical confinement [19, 20, 46]. This novel “bion” mechanism has been extended to fermions in other representations [47–49]. For related works on instanton-monopoles and calorons, see Refs. [50–67]².

Other diverse applications of twisted boundary conditions (imaginary chemical potential) to QCD can be found in Refs. [68–73].

In this paper, motivated by these intriguing developments, we embark on the first systematic study of QCD(adj) on $\mathbb{R}^3 \times S^1$ with a twisted boundary condition (1.1). Here S^1 is a compactified *spatial* direction.³ As the physics is periodic in ϕ modulo 2π it is sufficient to consider $0 \leq \phi \leq \pi$. Despite a tremendous amount of literature on QCD(adj) with ABC ($\phi = \pi$) and PBC ($\phi = 0$), studies on intermediate ϕ are quite limited; we are only aware of partial perturbative analyses at one loop [36, 38, 74] and a qualitative discussion by Shuryak [75]. Intuitively, the effect of ϕ is anticipated to be negligible on large S^1 . By contrast it has a dramatic impact on small S^1 : the system is in an Abelian confining phase at $\phi = 0$ and in a hot deconfined plasma phase at $\phi = \pi$. How do these phases compete with each other at intermediate ϕ ? Is Ünsal’s bion mechanism of confinement still operative at nonzero ϕ ? We address these questions in this work.

The realization of chiral symmetry is another important issue. Due to asymptotic freedom, the coupling $g(L)$ is small at $L \ll \Lambda_{\text{QCD}}^{-1}$ and chiral symmetry will be restored there. What happens at intermediate L is nontrivial. Based on the fact that the lowest Matsubara frequency of fermions obeying (1.1) is ϕ/L , one may naively expect that fermions become more relevant for smaller ϕ in the IR, leading to enhanced chiral symmetry breaking. It turns out, however, that this simple picture has to be modified because the Polyakov loop background shifts the net Matsubara frequency of fermions. Given that chiral dynamics is intertwined with center symmetry realization, it is essential for us to incorporate both at the same time for a correct understanding of the phase diagram.

One more remark is in order regarding the fate of center symmetry at intermediate L . In QCD(adj) with $N_f^W = 1$ (SYM), the partition function with $\phi = 0$ is nothing but the Witten index and is independent of L [14], hence one expects no center-symmetry-changing transition at $0 < L < \infty$. In QCD(adj) with $N_f^W \geq 2$ and $\phi = 0$, center

²Confusingly, the objects called ‘monopoles’ or ‘monopole-instantons’ in Refs. [43, 44, 59] are called ‘dyons’ in Refs. [56, 58, 60, 64, 65]. In this paper we will conform to the nomenclature of Refs. [43, 44, 59] for the reason in Ref. [21, footnote 6]. Mutual relationship and (in)consistency of these works are discussed in Ref. [21, Section 4].

³At $\phi = \pi$ the system is equivalent to a thermal field theory at temperature $T = 1/L$. Otherwise, we shall always view the compactified direction as a spatial direction, so all the phase transitions observed should be considered as zero-temperature quantum phase transitions. Note also that the VEV of a Polyakov loop that winds around a *spatial* direction does not distinguish the physical confined/deconfined phases, because it is no longer related to the thermal free energy of excitations. Nevertheless, just for the sake of convenience, we will continue calling a center-symmetric (center-broken) phase a “confined” (“deconfined”) phase, respectively.

symmetry is preserved at least for small L (by one-loop effects) and large L (by non-perturbative effects), but it is presently unclear if these domains are connected without any center-changing phase transition or not. If such a continuity were proven, it would mark significant progress towards a first-principle understanding of IR renormalons in QCD, as advocated in recent applications of resurgence theory to QFT [76–79]. However, lattice simulations [37, 38] as well as a model analysis [80] suggest that, in SU(3) QCD(adj) with light fermions at $\phi = 0$, there appears a center-broken phase at intermediate L , which calls into question the conjectured continuity between small L and large L . It also implies that the large- N volume independence [81, 82], whose premise is unbroken center symmetry, may fail at intermediate L . Can we rescue the continuity by changing the gauge group to SU(2) or by considering a phase diagram on the (L, ϕ) -plane? Answering this question constitutes part of the motivation of this work.

To address a number of important issues raised above, we combine perturbation theory, the index theorem, semiclassical methods and a chiral effective model to investigate the phase structure of QCD(adj) as a function of L , ϕ , and the fermion mass m . Our main focus is on $N_c = 2$ and $N_f^W = 2$, while the other cases are only briefly discussed. On the phase diagram we find a number of quantum phase transition lines that separate phases with or without chiral and center symmetry breaking. Consistency of obtained results with our knowledge on the limiting cases ($\phi = 0$, $\phi = \pi$ and $L \rightarrow 0$) is carefully examined, and the possibility of adiabatic continuity between the small- L Abelian phase and the large- L non-Abelian phase is scrutinized. All predictions in this work can be tested in future lattice simulations.

This paper is organized as follows. In Section 2 we focus on the center symmetry realization. In Section 2.1 we study center phase transitions in SU(2) and SU(3) gauge theories with twisted boundary conditions by using a one-loop effective potential, which is reliable for $L \ll \Lambda_{\text{QCD}}^{-1}$. In Section 2.2 we investigate the center phase structure by using a minimal non-perturbative gluon effective potential that reproduces the deconfinement transition in pure Yang-Mills theory. By varying m we interpolate between pure Yang-Mills theory ($m = \infty$) and massless QCD(adj) and delineate the evolution of the phase diagram. In Section 3 we use the Polyakov–Nambu–Jona-Lasinio (PNJL) model [83–85] to examine the influence of spontaneous chiral symmetry breaking on the phase structure of QCD(adj) in the chiral limit. First, we employ the high-temperature expansion to grasp qualitative features of the phase diagram and show that the Polyakov loop strongly affects chiral symmetry realization at $\phi \neq 0$. Then we move on to numerical analysis of the PNJL model, showing that the incorporation of chiral symmetry breaking modifies the phase diagram in a qualitative way. Among others, we find that the confining phase at $L \ll \Lambda_{\text{QCD}}^{-1}$ could be *disconnected* from the confining phase at $L \gg \Lambda_{\text{QCD}}^{-1}$ on the plane spanned by L^{-1} and ϕ , depending on the parameters of the model. Section 4 is devoted to summary and discussions. In Appendix A, we analyze zero modes of the Dirac operator on $\mathbb{R}^3 \times S^1$ for general ϕ on the basis of the index theorem in Refs. [86, 87]. In Appendix B we review preceding studies on chiral effective models pertinent to the present work.

2 Center symmetry realization

2.1 Phase structure at small S^1

In this section we discuss center and gauge symmetry breaking at small S^1 using perturbation theory and semiclassical methods. In $SU(N)$ QCD(adj), the one-loop β function of the running coupling is given by [88]

$$\beta(g) = -\frac{g^3 N}{(4\pi)^2} \left(\frac{11}{3} - \frac{2}{3} N_f^W \right), \quad (2.1)$$

so the asymptotic freedom requires $N_f^W \leq 5$. We will use N and N_c interchangeably to denote the number of colors in the rest of this paper.

In considering a twisted boundary condition, one needs to carefully distinguish even N_f^W and odd N_f^W . For simplicity let us begin with $N_f^W = 1$, with a boundary condition $\lambda(\vec{x}, x_4 + L) = e^{i\phi} \lambda(\vec{x}, x_4)$ for the adjoint Weyl fermion λ . As discussed in Ref. [87, Section 5.2] (see also Refs. [89, 90]), fermions in this setup induce a Chern-Simons term in the three-dimensional effective theory on small S^1 , whose coefficient depends on ϕ . As is well known, the coefficient of the Chern-Simons term has to be properly quantized in order to maintain the invariance under large gauge transformations. It then follows that ϕ *must be an integer multiple of π/N* [87]; otherwise the gauge symmetry is spoiled and the theory is inconsistent.

There is an intuitive way to see why only discrete values of ϕ are allowed. First, let us recall that the angle ϕ can be mapped to an imaginary chemical potential by field redefinition. Hence the partition function may be cast into the form

$$Z(\phi) = \text{Tr} [e^{-LH - i(\phi + \pi)N_F}], \quad (2.2)$$

where H is the Hamiltonian and N_F is the fermion number. At $\phi = \pi$ it reduces to the thermal partition function $\text{Tr} [e^{-LH}]$, as it should. Now what is problematic with (2.2) is that N_F is not a conserved quantity: the $U(1)$ fermion number symmetry at the classical level is broken to \mathbb{Z}_{2N} by instantons. Since N_F is conserved only modulo $2N$, the expression (2.2) is ill-defined, unless $(\phi + \pi) \cdot 2N$ is an integer multiple of 2π . This leads to the quantization condition of Ref. [87]. By the same token, for QCD(adj) with $N_f^W \geq 2$ Weyl fermions of one chirality, the gauge invariance of the partition function requires that ϕ be an integer multiple of $\pi/(NN_f^W)$. It is thus impossible to vary ϕ smoothly.

However, when N_f^W is even, there is a way to avoid this pathology. By judiciously assigning $+\phi$ to $N_f^W/2$ Weyl fermions and $-\phi$ to the other $N_f^W/2$ Weyl fermions, the Chern-Simons term can be made to vanish after cancellation. This will happen automatically if we combine all the Weyl fermions into $N_f^D (= N_f^W/2)$ Dirac fermions, and impose a twisted boundary conditions (1.1) on the latter. For this reason we will only consider Dirac fermions in the rest of this paper.⁴

⁴More generally, one should embed the $U(1)$ boundary condition of fermions into a non-Abelian flavor symmetry that is anomaly free. This prescription works for odd N_f^W as well. We are grateful to M. Ünsal for pointing out this to us.

QCD(adj) is asymptotically free for $N_f^W \leq 5$, hence $N_f^D = 1$ or 2 . Recent lattice simulations for SU(2) indicate that both $N_f^D = 1$ and 2 may reside in the conformal window [91–96], contrary to old simulations where chiral symmetry breaking was observed [1, 2]. As for SU(3), $N_f^D = 2$ is likely to be outside the conformal window [3, 4, 37, 38], but there are uncertainties [97, 98]. The lattice data on the large- N limit [99–104] are not conclusive yet.

Although our discussion in Section 2.1 is unaffected by the absence or presence of IR conformality, Sections 2.2 and 3 which concern non-perturbative aspects of QCD(adj) can be influenced by the location of the conformal window. Because the determination of the conformal window itself is not the purpose of this work, in Sections 2.2 and 3 we will use effective models for specific values of N and N_f^D where chiral symmetry breaking and confinement are simply *assumed to occur* on \mathbb{R}^4 . After fixing the model parameters this way we will move on to the discussion of how the phase structure varies with ϕ . Thus our model analysis should never be taken as constraining the range of conformal window.

In the remainder of Section 2.1, we delineate the phase structure and dynamics at $L \ll \Lambda_{\text{QCD}}^{-1}$ using a perturbative potential and semiclassics. We will refer to a center-symmetric phase as a “confined” phase and to a center-broken phase as a “deconfined” phase, with caveats of footnote 3 in mind.

2.1.1 One-loop effective potential

In this section we summarize the one-loop effective potential for the Polyakov loop holonomy in SU(N_c) gauge theories on $\mathbb{R}^3 \times S^1$ with N_f^D adjoint Dirac fermions with a twisted boundary condition (1.1). Here we assemble relevant formulas for readers’ convenience; full derivations can be found elsewhere [36, 38, 74].

To obtain the effective potential for the Polyakov loop holonomy, one needs to evaluate the functional determinant with a constant background field along the compact direction [105, 106]

$$\langle A_4 \rangle = \frac{1}{L} \text{diag}(q_1, q_2, \dots, q_{N_c}) \quad \text{with} \quad \sum_{k=1}^{N_c} q_k = 0. \quad (2.3)$$

The holonomy Ω and the normalized traced Polyakov loop in the fundamental representation P_F are defined by

$$\Omega \equiv \mathcal{P} \exp \left(i \oint dx_4 A_4 \right) \quad \text{and} \quad P_F \equiv \frac{1}{N_c} \text{Tr} \Omega, \quad (2.4)$$

where \mathcal{P} denotes path-ordering. The gluon+ghost contribution to the one-loop effective potential \mathcal{V}_g reads

$$\mathcal{V}_g(N_c, L; \{q\}) = -\frac{2}{\pi^2 L^4} \sum_{n=1}^{\infty} \frac{1}{n^4} \text{Tr}_{\text{adj}}(\Omega^n) \quad (2.5)$$

$$= -\frac{2}{\pi^2 L^4} \sum_{n=1}^{\infty} \frac{1}{n^4} \sum_{i,j=1}^{N_c} \left(1 - \frac{1}{N_c} \delta_{ij} \right) \cos(nq_{ij}), \quad (2.6)$$

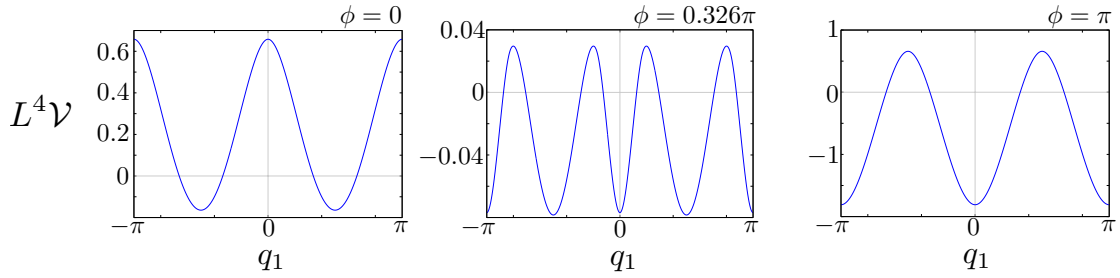


Figure 1. $\mathcal{V}(N_c = 2, N_f^D = 1)$ in (2.9) at $m = 0$ for three values of ϕ . A first-order phase transition is seen to occur at $\phi \simeq 0.326\pi$.

with $q_{ij} \equiv q_i - q_j$.

The adjoint fermion contribution consists of a “zero-temperature” part \mathcal{V}_χ and a “thermal” part \mathcal{V}_{adj} .⁵ As \mathcal{V}_χ has no $\{q\}$ -dependence it can be dropped throughout Section 2. (It will be retrieved later in Section 3 where we discuss spontaneous chiral symmetry breaking.) \mathcal{V}_{adj} is given by

$$\begin{aligned} \mathcal{V}_{\text{adj}}(N_c, N_f^D, L, m, \phi; \{q\}) &= \frac{N_f^D m^2}{\pi^2 L^2} \sum_{n=1}^{\infty} \frac{K_2(nLm)}{n^2} [e^{in\phi} \text{Tr}_{\text{adj}}(\Omega^n) + e^{-in\phi} \text{Tr}_{\text{adj}}(\Omega^{\dagger n})] \end{aligned} \quad (2.7)$$

$$= \frac{2N_f^D m^2}{\pi^2 L^2} \sum_{n=1}^{\infty} \frac{K_2(nLm)}{n^2} \sum_{i,j=1}^{N_c} \left(1 - \frac{1}{N_c} \delta_{ij}\right) \cos(n(q_{ij} + \phi)), \quad (2.8)$$

where m is the fermion mass, $0 \leq \phi \leq \pi$ is the boundary twist, and $K_\nu(x)$ is the modified Bessel function of the second kind. As a small consistency check, we verify that $\mathcal{V}_g + \mathcal{V}_{\text{adj}}$ vanishes exactly for $\phi = 0$, $N_f^D = 1/2$ and $m \rightarrow 0$, as expected from supersymmetry.

2.1.2 Phase diagram for $(N_c, N_f^D) = (2, 1)$, $(3, 1)$ and $(3, 2)$

Let us begin with SU(2) QCD(adj) with $N_f^D = 1$. The one-loop effective potential in this case is given by

$$\mathcal{V}(N_c = 2, N_f^D = 1) = \mathcal{V}_g(N_c = 2, L; \{q\}) + \mathcal{V}_{\text{adj}}(N_c = 2, N_f^D = 1, L, m, \phi; \{q\}), \quad (2.9)$$

with the condition $q_1 + q_2 = 0$. The potential $L^4 \mathcal{V}(N_c = 2, N_f^D = 1)$ in the massless limit ($m = 0$) is plotted in Figure 1 for $-\pi \leq q_1 \leq \pi$. For $0 \leq \phi < 0.326\pi$, the global minima are located at $(q_1, q_2) = (\pm\pi/2, \mp\pi/2)$, thus the VEV of the Polyakov loop is

$$\langle P_F \rangle = \frac{1}{2} \text{Tr} \begin{pmatrix} e^{\pm i\pi/2} & 0 \\ 0 & e^{\mp i\pi/2} \end{pmatrix} = 0, \quad (2.10)$$

which indicates that the \mathbb{Z}_2 center symmetry is intact in this phase. It is also notable that the SU(2) gauge symmetry is broken to U(1) since $q_1 \neq q_2$. At $\phi \sim 0.326\pi$ there is a

⁵We once again emphasize that this terminology is used only for convenience; S^1 in this work is considered as a compact spatial direction.

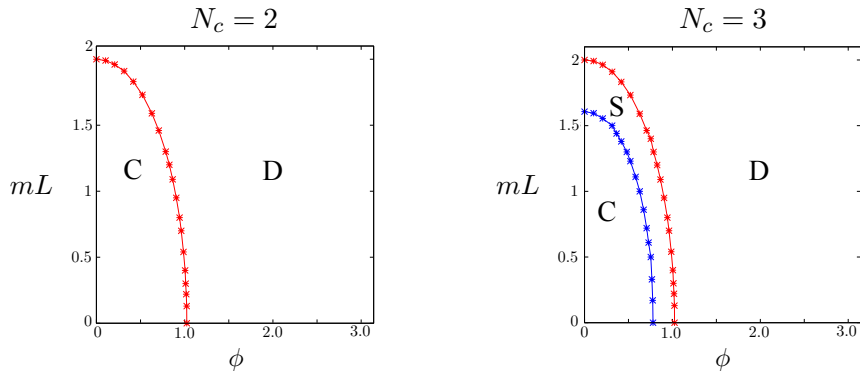


Figure 2. The mL - ϕ phase diagram (**Left:** $N_c = 2$, $N_f^D = 1$. **Right:** $N_c = 3$, $N_f^D = 1$). The symbols C, D and S refer to the confining phase, the deconfined phase and the split phase, respectively. In both figures, the transitions are first order.

first-order phase transition to the vacuum with $(q_1, q_2) = (0, 0)$ and $(\pm\pi, \mp\pi)$, for which

$$\langle P_F \rangle = \frac{1}{2} \text{Tr} \begin{pmatrix} \pm 1 & 0 \\ 0 & \pm 1 \end{pmatrix} = \pm 1. \quad (2.11)$$

This phase breaks \mathbb{Z}_2 spontaneously but preserves the $SU(2)$ gauge symmetry. In summary, the phase structure for $m = 0$ is given as follows:

$(N_c, N_f^D) = (2, 1)$	Phase	$\langle P_F \rangle$	Gauge sym.
$0 \leq \phi < 0.326\pi$	Confined	0	U(1)
$0.326\pi < \phi \leq \pi$	Deconfined	± 1	SU(2)

(2.12)

Our result is consistent with Ref. [36, Theorem 5].

For $m \neq 0$, the shape of the potential (2.9) depends on ϕ and Lm . As shown in Figure 2 (left), the confining phase is favored for small Lm and small ϕ , whereas the deconfined phase is favored throughout the rest of the phase diagram. This can be qualitatively understood from the fact that the adjoint fermions decouple from the low-energy physics when either the current mass or the lowest Matsubara frequency $\sim \phi/L$ is large, leaving gluons that favor the deconfined phase at small S^1 .

Next, we consider $SU(3)$ QCD(adj) with $N_f^D = 1$. The one-loop effective potential for this case is given by

$$\mathcal{V}(N_c = 3, N_f^D = 1) = \mathcal{V}_g(N_c = 3, L; \{q\}) + \mathcal{V}_{\text{adj}}(N_c = 3, N_f^D = 1, L, m, \phi; \{q\}), \quad (2.13)$$

with the condition $q_1 + q_2 + q_3 = 0$. For massless case $m = 0$, the potential $L^4 \mathcal{V}(N_c = 3, N_f^D = 1)$ is depicted in Figure 3 as a function of $-\pi \leq q_1, q_2 \leq \pi$ and ϕ . For $0 \leq \phi < 0.248\pi$, the global minima are given by the six permutations of $(q_1, q_2, q_3) = (0, 2\pi/3, -2\pi/3)$, and

$$\langle P_F \rangle = \frac{1}{3} \text{Tr} \begin{pmatrix} 1 & 0 & 0 \\ 0 & e^{2i\pi/3} & 0 \\ 0 & 0 & e^{-2i\pi/3} \end{pmatrix} = 0. \quad (2.14)$$

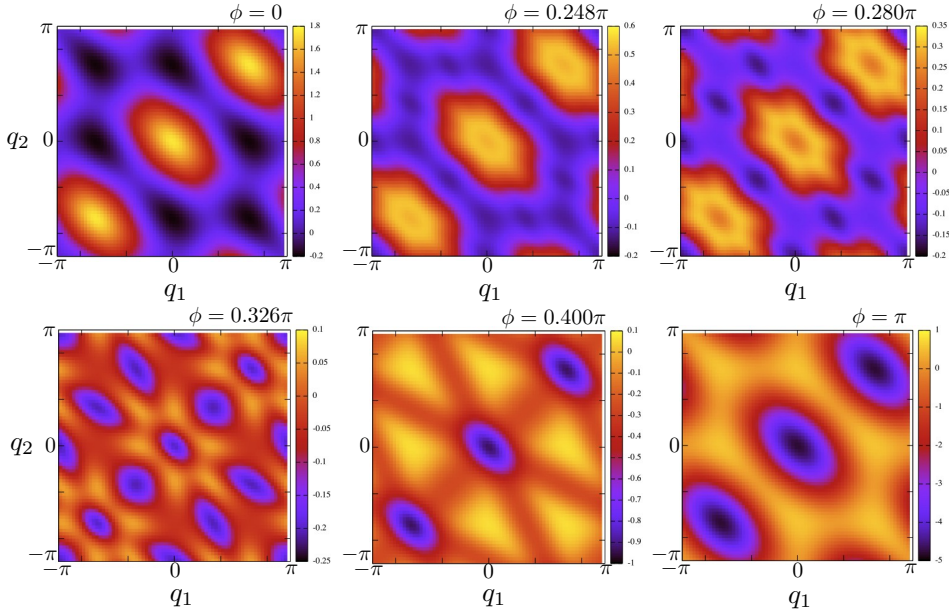


Figure 3. Contour plots of $\mathcal{V}(N_c = 3, N_f^D = 1)$ in (2.13) at $m = 0$ and $\phi \in \{0, 0.248\pi, 0.280\pi, 0.326\pi, 0.400\pi, \pi\}$. Phase transitions occur at $\phi \simeq 0.248\pi$ and $\phi \simeq 0.326\pi$, from the confining to the split phase and then to the deconfined phase, respectively.

This phase is \mathbb{Z}_3 -symmetric but breaks the $SU(3)$ gauge symmetry down to $U(1) \times U(1)$. At $\phi \sim 0.248\pi$ there is a first-order phase transition to the vacuum with $(q_1, q_2, q_3) = (0, \pm\pi, \mp\pi), (\pm 2\pi/3, \mp\pi/3, \mp\pi/3)$ and their permutations, for which

$$\langle P_F \rangle = -\frac{1}{3}, \frac{e^{i\pi/3}}{3}, \text{ and } \frac{e^{-i\pi/3}}{3}. \quad (2.15)$$

This is the so-called “split phase” [37, 74] in which $SU(3)$ gauge symmetry is broken to $SU(2) \times U(1)$ since only two of the eigenvalues of the holonomy are degenerate. The \mathbb{Z}_3 symmetry is also broken by $\langle P_F \rangle \neq 0$. Finally, at $\phi \sim 0.326\pi$ there is another first-order phase transition to the vacuum with $(q_1, q_2, q_3) = (0, 0, 0)$ and $(\pm 2\pi/3, \pm 2\pi/3, \pm 2\pi/3)$, with the Polyakov loop VEV

$$\langle P_F \rangle = 1, e^{2i\pi/3}, \text{ and } e^{-2i\pi/3}. \quad (2.16)$$

This is the usual deconfined phase. The overall center phase structure for $m = 0$ is summarized below. We note that a similar phase structure has been observed in pure Yang-Mills theory with deformation [107].

$(N_c, N_f^D) = (3, 1)$	Phase	$\langle P_F \rangle$	Gauge sym.
$0 \leq \phi < 0.248\pi$	Confined	0	$U(1) \times U(1)$
$0.248\pi < \phi < 0.326\pi$	Split	$-1/3, e^{\pm i\pi/3}/3$	$SU(2) \times U(1)$
$0.326\pi < \phi \leq \pi$	Deconfined	$1, e^{\pm 2i\pi/3}$	$SU(3)$

(2.17)

For $m \neq 0$, the potential (2.13) depends on Lm . The phase structure, depicted in Figure 2 (right), is analogous to the $SU(2)$ case as a whole. It is intriguing that the confined and the deconfined phases are always separated by the split phase, although no such

intermediate phase appears around the finite-temperature transition in QCD(adj). As N_c is increased there will be even more exotic phases with broken gauge symmetry, between the confined phase at $\phi = 0$ and the deconfined phase at $\phi = \pi$.

Finally let us briefly discuss the case with $N_c = 3$ and $N_f^D = 2$, for which we only show the result for $m = 0$ below. This result is consistent with Ref. [38, eq. (4.11)].

$(N_c, N_f^D) = (3, 2)$	Phase	$\langle P_F \rangle$	Gauge sym.
$0 \leq \phi < 0.319\pi$	Confined	0	$U(1) \times U(1)$
$0.319\pi < \phi < 0.416\pi$	Split	$-1/3, e^{\pm i\pi/3}/3$	$SU(2) \times U(1)$
$0.416\pi < \phi \leq \pi$	Deconfined	$1, e^{\pm i2\pi/3}$	$SU(3)$

(2.18)

While the overall phase structure is the same as the previous $N_f^D = 1$ case, the confined (deconfined) phase has enlarged (shrunk), as there are more fermions that tend to favor the confining phase at small ϕ .

We here comment on the validity and limitation of the perturbative one-loop effective potential. The method may be used to calculate the leading order contribution to the free energy and determine the phase structure at least in the weak-coupling regime with $L \ll \Lambda_{\text{QCD}}^{-1}$. However perturbation theory is not only blind to the strong-coupling physics such as chiral symmetry breaking and confinement on large L but also misses a plethora of non-perturbative phenomena induced by topological objects at small ϕ for $L \ll \Lambda_{\text{QCD}}^{-1}$. We will discuss the latter in the next subsection.

2.1.3 Mass gap and confinement from semiclassics

Before considering QCD(adj) at general ϕ , let us recapitulate the semiclassical physics of QCD(adj) at $\phi = 0$ following Refs. [43, 44]. In this subsection we always assume that the bare mass of fermions is zero.

First of all, in QCD at high temperature $T \gg \Lambda_{\text{QCD}}$, the coupling goes small due to asymptotic freedom and the semiclassical instanton gas approximation is justified [105]. On the other hand, the magnetic sector remains strongly coupled at any T : the fermions with ABC decouple from the dynamics at high T and the theory reduces to the three-dimensional Yang-Mills theory, which generates non-perturbative mass gap and exhibits an area law of confinement for the spatial Wilson loop, precluding a naive application of perturbation theory.

The situation is drastically different if we go to QCD(adj) with PBC at small S^1 . The major differences, as compared to thermal QCD, are as follows.⁶

- The adjoint fermions with PBC stabilizes a confining phase at small L , as shown in Section 2.1.2. They never decouple in the IR since they have a zero mode along S^1 .
- The $SU(N)$ gauge symmetry is broken to $U(1)^{N-1}$ and as a result of which, the off-diagonal components of the gauge fields and fermions acquire a large mass $\sim 1/L$

⁶See Ref. [66] for a nice review on this subject.

via the Higgs mechanism. For $N_f^W \geq 2$, the electric gluons A_4^a also acquire a mass $\sim g/L$ from the one-loop effective potential.

- The perturbative low-energy effective theory on \mathbb{R}^3 consists of massless photons and fermions, which are neutral under $U(1)^{N-1}$ and hence non-interacting. Since charged particles are absent below the scale $\sim 1/L$, the running coupling $g(\mu)$ ceases to run at $\mu \sim 1/L$; $g(1/L)$ is small provided $1/L \gg \Lambda_{\text{QCD}}$ ⁷ and validates the semiclassical expansion.
- In the background of \mathbb{Z}_N -symmetric Polyakov loop, instantons split into $N - 1$ BPS monopoles and one KK monopole [51–53], which interact with each other via a 3d Coulomb potential. They are more relevant than instantons due to their smaller action $\left(S_0 = \frac{8\pi^2}{g^2 N} < \frac{8\pi^2}{g^2}\right)$.
- Monopoles alone do *not* contribute to the bosonic potential, because each monopole is accompanied by 2 fermionic zero modes (per flavor) in accordance with the Index theorem. (This is to be contrasted with Polyakov’s 3d $U(1)$ model [45] where the monopoles do generate a mass gap.) Instead, it is the bound states of BPS and $\overline{\text{KK}}$ monopoles called *magnetic bions*⁸, that generate a mass gap of order $L^{-1} e^{-S_0}$ for photons [43, 44]. They are topologically neutral and carry magnetic charge 2. It is the attractive interaction due to massless fermion exchange that overcomes the Coulomb repulsion between BPS and $\overline{\text{KK}}$ monopoles, leading to the formation of molecules.

Now we are prepared to ask what occurs when $\phi \neq 0$. As shown in the last subsection, the confining phase with $\langle P_F \rangle = 0$ is sustained for $0 \leq \phi < \phi_c$ for some critical ϕ_c which depends on N and N_f^D . In this phase, the Polyakov-loop holonomy is \mathbb{Z}_N -symmetric and breaks the $SU(N)$ gauge symmetry down to $U(1)^{N-1}$, in much the same way as at $\phi = 0$. But a new feature shows up in the three-dimensional perturbative effective theory⁹:

$$S_{\text{eff}} = \int_{\mathbb{R}^3} d^3x \frac{L}{g^2} \sum_{\ell=1}^{N-1} \left[\frac{1}{4} F_{ij}^{(\ell)2} + \sum_{f=1}^{N_f^D} \overline{\Psi}_f^{(\ell)} \left(\gamma_i \partial_i + i \frac{\phi}{L} \gamma_4 \right) \Psi_f^{(\ell)} \right], \quad (2.19)$$

with $i, j = 1, 2, 3$ denoting the three spatial directions. Here $\Psi_f^{(\ell)}$ are adjoint Dirac spinors with ℓ labeling the diagonal components, and the term $\propto \phi/L \equiv m_\psi$ originates from the twisted boundary condition.¹⁰ The latter is often called “real mass” to distinguish it from the complex Dirac mass. For this effective theory to be valid, the cutoff scale μ must satisfy $m_\psi \ll \mu \ll g/L$, which necessitates $\phi \ll g$. If $\phi = \mathcal{O}(1)$, fermions are integrated out as well, and one ends up with a theory of free massless photons. So much for the perturbation theory.

⁷Here we assume $N = \mathcal{O}(1)$. In general, a weak-coupling analysis is valid if $N L \Lambda_{\text{QCD}} \ll 1$ [82].

⁸This is a simplified statement valid for $SU(2)$. For general $SU(N)$, precisely speaking, a “magnetic bion” is a bound state of a monopole of type i and an anti-monopole of type $i + 1$ for $i = 1, \dots, N$ [44].

⁹In this subsection we assume $0 \leq \phi < \phi_c < \pi$. Formulas valid for generic ϕ can be easily obtained from those in this subsection by replacing ϕ with the lowest Matsubara frequency, i.e., $\min\{2\pi n + \phi \mid n \in \mathbb{Z}\}$.

¹⁰This term was used in Ref. [108] as an IR regulator for fermions.

Now we turn to the non-perturbative dynamics. Associated with the gauge symmetry breaking, there appear N types of monopoles ($N - 1$ BPS and one KK). On \mathbb{R}^3 each BPS monopole carries $2N_f^W$ adjoint zero modes (2 per flavor), as dictated by the Callias index theorem. On $\mathbb{R}^3 \times S^1$ the index generally depends on the boundary condition ϕ , but as will be shown in Appendix A, the number of adjoint zero modes on each monopole is *independent of ϕ* and equals $2N_f^W$ for the particular case of a \mathbb{Z}_N -symmetric Polyakov-loop background. (See the left panel of Figure 14 in Appendix A, where the index at $q = \pi/2$ is equal to 2 for all values of ϕ .) This implies that, for $0 \leq \phi < \phi_c$, monopoles interact with each other via a sum of a Coulomb potential and an attractive potential induced by fermion zero-mode exchange. This picture is essentially the same as at $\phi = 0$.

To see a new phenomenon specific to $\phi \neq 0$, let us turn to the expression for the bion amplitude [44, 66, 77]

$$Z_{\text{bion}}(g) \sim \frac{1}{g^8} \exp\left(-\frac{2}{N} \frac{8\pi^2}{g^2} (1 + cg)\right) \int d^3x \int d^3y \exp\left(-\frac{4\pi L}{g^2 |\vec{x} - \vec{y}|}\right) [S_F(\vec{x} - \vec{y})]^{2N_f^W}, \quad (2.20)$$

where the factor $1/g^8$ is associated with the Jacobian for collective coordinates, the first exponential is the weight for two monopoles (with a correction $\propto cg$, $c = \mathcal{O}(1)$, arising from the non-BPS nature of monopoles [109]), the second exponential is the Coulomb interaction between monopoles located at \vec{x} and \vec{y} , and the final factor is the fermion zero-mode exchange interaction, which can be extracted from the correlator of 't Hooft vertices [44].¹¹ The free fermion propagator S_F is defined as

$$S_F(\vec{r}) \equiv \int \frac{d^3p}{(2\pi)^3} \frac{e^{i\vec{p}\cdot\vec{r}}}{\sigma_i p_i + im_\psi} \Big|_{m_\psi = \phi/L} \quad (2.21)$$

$$= \frac{i}{4\pi} e^{-m_\psi r} \left\{ \left(\frac{1}{r^3} + \frac{m_\psi}{r^2} \right) \sigma_i x_i - \frac{m_\psi}{r} \mathbb{1} \right\}, \quad (2.22)$$

where the higher Matsubara frequencies are not relevant to our argument and are omitted above. Due to the real mass m_ψ , the fermion propagator has an exponential fall-off at large r . At this point we emphasize the difference between the real mass m_ψ and the complex Dirac and Majorana masses; the former does not yield a disconnected piece for the 't Hooft vertex correlator, whereas the latter soak up zero modes of monopoles and allow unpaired monopoles to contribute to the bosonic potential [21].

Making a crude approximation $S_F(\vec{r}) \sim e^{-m_\psi r}$, one finds

$$Z_{\text{bion}} \sim \frac{1}{g^8} \exp\left(-\frac{2}{N} \frac{8\pi^2}{g^2} (1 + cg)\right) \int_{r_{\min}}^{\infty} dr r^2 \exp(-V_{\text{eff}}(r)), \quad (2.23)$$

where $r_{\min} \sim L$ is a cutoff¹² (irrelevant for the following discussion) and

$$V_{\text{eff}}(r) = \frac{4\pi L}{g^2 r} + 2N_f^W m_\psi r. \quad (2.24)$$

¹¹In (2.20) we are a bit cavalier about spinor indices but this is inessential to the ensuing discussion.

¹²The integral is convergent even if r_{\min} is set to zero; however, the interaction between monopoles at short distance cannot be approximated by a Coulomb potential and the argument based on (2.24) loses its meaning.

The minimum of $V_{\text{eff}}(r)$ is located at $r = r_b$ with

$$r_b \equiv \sqrt{\frac{2\pi L}{g^2 N_f^W m_\psi}} = \sqrt{\frac{2\pi}{N_f^W \phi}} \frac{L}{g}. \quad (2.25)$$

This gives a rough size of bions. It is noteworthy that r_b is *far smaller* than the bion size $\sim L/g^2$ at $\phi = 0$ [66, 77]. This is because the linear confining potential $\sim m_\psi r$ in $V_{\text{eff}}(r)$ binds monopoles more strongly than the logarithmic potential $\sim \log(m_\psi r)$ that acts at $\phi = 0$. This mechanism is reminiscent of the instanton–anti-instanton molecules in QCD at high temperature, where the zero-mode exchange induces a linear potential between instantons and anti-instantons [110, 111].

Now let us perform three consistency checks:

- $r_b \gg L$ for $\phi = \mathcal{O}(1)$, so the usage of the Coulomb potential is valid.
- $\log(m_\psi r_b) \ll m_\psi r_b$ implies that the linear potential is indeed the dominant part of the interaction of monopoles on the scale $r \approx r_b$, which justifies our approximation.
- In the above treatment the electric interaction of monopoles has been ignored. This simplification is innocuous at $\phi = 0$ because the distance between monopoles $\sim L/g^2$ is much longer than the inverse of the gap $\sim g/L$ of A_4 . By contrast, at $\phi \neq 0$, r_b^{-1} is comparable to the gap of A_4 and, precisely speaking, the A_4 -exchange interaction could be as important as the other interactions. In Ref. [77, eq. (5.10)] a full effective potential between monopoles incorporating the electric interaction has been worked out, where A_4 -exchange modifies the $\mathcal{O}(1)$ prefactor of the Coulomb interaction, but never changes an overall form of the potential. On the basis of this observation, we conclude that the electric interaction would not invalidate our argument here, even though it may well change the $\mathcal{O}(1)$ prefactor of L/g in (2.25).

In order to evaluate the integral (2.23) we switch to the dimensionless variable $x \equiv r/r_b$, finding

$$Z_{\text{bion}} \sim \frac{1}{g^8} \exp\left(-\frac{2}{N} \frac{8\pi^2}{g^2} (1+cg)\right) (r_b)^3 \int_{x_{\min}}^{\infty} dx x^2 \exp\left(-\frac{2\sqrt{2\pi N_f^W \phi}}{g} \left(x + \frac{1}{x}\right)\right). \quad (2.26)$$

The integral is dominated by the contribution from $x \approx 1$. Performing a gaussian approximation around $x = 1$, which is accurate for $g \ll 1$, we finally obtain

$$Z_{\text{bion}} \sim \frac{1}{\phi^{7/4} g^{21/2}} \exp\left(-\frac{2}{N} \frac{8\pi^2}{g^2} (1+cg) - \frac{4\sqrt{2\pi N_f^W \phi}}{g}\right). \quad (2.27)$$

This result is valid regardless of whether N_f^W is inside the conformal window or not. As is evident from (2.27), the emergence of the factor $\sim 1/g$ in the exponent shows that the bions at $\phi \neq 0$ are *exponentially suppressed* compared to the case at $\phi = 0$.¹³ An intuitive

¹³The contribution due to $\phi \neq 0$ in the exponent is parametrically of the same order as the correction from cg ; this is the reason why we have kept the latter in all equations so far.

explanation for this is that, owing to the strong binding force between monopoles, they are brought closer together and feel the Coulomb repulsion more severely than at $\phi = 0$, which makes bions energetically costlier. A natural question to ask is: when does this mechanism set in if ϕ is smoothly increased from 0? The linear potential due to the exchange of massive fermions will begin to matter only when $m_\psi^{-1} = L/\phi$ becomes comparable to the bion size L/g^2 . This suggests that the bion suppression sets in for $\phi \gtrsim g^2$.

Alongside the dilution of bions, the bion-induced non-perturbative quantities such as the mass gap and the spatial string tension are also expected to be exponentially suppressed compared to $\phi = 0$. To see this, let us compute the mass gap \mathcal{M} of photons following Refs. [45, 66] for $N = 2$. Using the two-loop running coupling

$$\frac{g(L)^2}{4\pi} = \frac{2\pi}{\beta_0 \log \frac{1}{L\Lambda}} \left(1 - \frac{\beta_1 \log \log(\frac{1}{L\Lambda})^2}{\beta_0^2 \log(\frac{1}{L\Lambda})^2} \right) \quad (2.28)$$

with $\beta_0 = (22 - 4N_f^W)/3$ and $\beta_1 = (136 - 64N_f^W)/3$, we obtain

$$\begin{aligned} \mathcal{M} &= 8\pi \sqrt{\frac{2Z_{\text{bion}}(g)}{g^2 L^2}} \quad (2.29) \\ &\sim \frac{\phi^{-\frac{7}{8}}}{L} \left(\log \frac{1}{L\Lambda} \right)^{\frac{25}{8} - \frac{\beta_1}{4\beta_0}} (L\Lambda)^{\beta_0/2} \exp \left(- \left(\sqrt{\frac{2\pi^2(N_f^W - 1)}{3}} + \sqrt{\frac{N_f^W \phi}{\pi}} \right) \sqrt{\beta_0 \log \frac{1}{L\Lambda}} \right), \quad (2.30) \end{aligned}$$

where we have substituted $c = \sqrt{\frac{N_f^W - 1}{3}}$ for $N = 2$ [109] and used Λ in place of Λ_{QCD} in order not to clutter the notation. While (2.30) looks fairly complicated, it is not difficult to see the leading behavior at $L\Lambda \ll 1$. For $N_f^W = 2$, we get $\beta_0 = 14/3$ and $\mathcal{M} \sim \frac{1}{L} (L\Lambda)^{\beta_0/2} \propto L^{4/3} \rightarrow 0$ as $L \rightarrow 0$. For $N_f^W = 4$, we get $\beta_0 = 2$ and the leading powers of L in (2.30) cancel exactly: the subleading factors then yield

$$\mathcal{M} \sim \left(\log \frac{1}{L\Lambda} \right)^{\frac{65}{8}} \exp \left(- \left(2\pi + \sqrt{\frac{8\phi}{\pi}} \right) \sqrt{\log \frac{1}{L\Lambda}} \right) \rightarrow 0 \quad \text{as } L\Lambda \rightarrow 0. \quad (2.31)$$

The mass gap therefore vanishes in both cases in the limit $L\Lambda \rightarrow 0$. This conclusion is the same as that for $\phi = 0$ [66], but the magnitude of \mathcal{M} is by orders of magnitude smaller, owing to the new factor $\exp \left(- \sqrt{\frac{8\phi}{\pi}} \sqrt{\log \frac{1}{L\Lambda}} \right) \ll 1$. The string tension γ associated with the ‘‘spatial’’ Wilson loop in \mathbb{R}^3 is also diminished at $\phi \neq 0$ by the same factor, because the latter is related to the mass gap as $\gamma \sim \frac{g^2}{L} \mathcal{M}$ [45, 66]. Such an exponential suppression of non-perturbative physics is the main conclusion of this subsection.

Final remark is in order concerning the low-energy limit of the theory. The photons will pick up one of the N degenerate minima of the bion-induced potential and the ground state will then break the \mathbb{Z}_N shift symmetry spontaneously [43, 44].¹⁴ Since fermions and photons are both massive, there are no massless particles in the spectrum and the IR limit

¹⁴This \mathbb{Z}_N symmetry must not be confused with the \mathbb{Z}_N center symmetry, which is unbroken for $0 \leq \phi \leq \phi_c$ at small L .

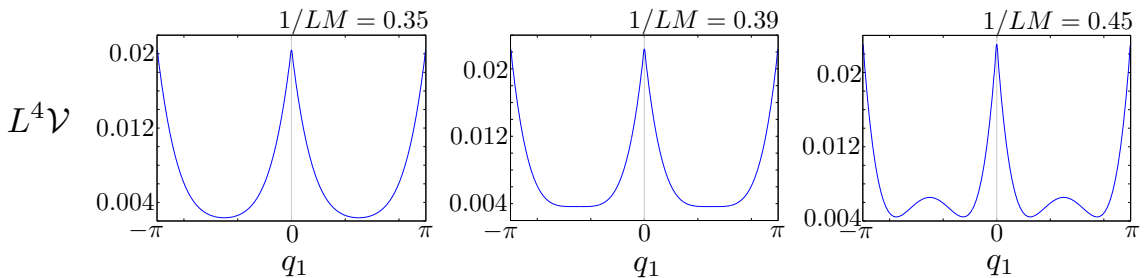


Figure 4. The non-perturbative potential $\mathcal{V}_g^{\text{np}}$ for $N_c = 2$ as a function of q_1 for $1/LM = 0.35$, 0.39 , and 0.45 . A second-order phase transition occurs at $1/LM \simeq 0.390$.

is trivial, as opposed to the case $\phi = 0$ where the spectrum contains *massless* fermions with unbroken chiral symmetry.

Other interesting topics not discussed in this subsection, such as neutral bions and bion-(anti-)bion molecules at $\phi \neq 0$ as well as their relevance to the resurgence theory and trans-series [76, 77], are deferred to future work.

2.2 Phenomenological gluonic potential

In Section 2.1 we worked out the phase structure of QCD(adj) on small S^1 using perturbation theory. This method cannot be extended to the region $L \gtrsim \Lambda_{\text{QCD}}^{-1}$ where the coupling is strong. To gain some insight into the center symmetry realization over the whole range $0 < L < \infty$, we shall in the following use a phenomenological gluonic potential that mimics characteristics of Yang-Mills theory as much as possible. Of course such a potential is not unique at all (see e.g., Ref. [112, Section 2] for comparisons). Here we require the potential to satisfy the following two conditions:

- It should agree with the one-loop potential $\mathcal{V}_g(N_c, L; \{q\})$ in (2.6) for sufficiently small L .
- It should reproduce the confinement/deconfinement phase transition of pure Yang-Mills theory at some scale $L^{-1} = T_d \sim \Lambda_{\text{QCD}}$, with the correct order of transition.

We take the following form that fulfills both requirements [80, 113]:

$$\mathcal{V}_g^{\text{np}}(N_c, M, L; \{q\}) = -\frac{2}{\pi^2 L^4} \sum_{n=1}^{\infty} \frac{1}{n^4} \left(1 - \frac{M^2 L^2}{4} n^2\right) \sum_{i,j=1}^{N_c} \left(1 - \frac{1}{N_c} \delta_{ij}\right) \cos(nq_{ij}), \quad (2.32)$$

where $M \sim \Lambda_{\text{QCD}}$ is a non-perturbative mass scale that controls the deconfinement transition temperature. One can easily check that $\mathcal{V}_g^{\text{np}}$ reduces to (2.6) as $ML \rightarrow 0$. Moreover it exhibits a second-order transition for $N_c = 2$ and a first-order transition for $N_c = 3$, in agreement with lattice simulations. In Figure 4 the potential for $N_c = 2$ is shown: the transition from a confining phase at small L^{-1} to a deconfined phase at large L^{-1} occurs at $L^{-1} \equiv T_d^{\text{YM}} \simeq 0.390M$.

From now, we discuss the center symmetry realization for $N_c = 2$ and $N_f^D = 1$ in the space of $1/L$, m and ϕ with this effective potential:

$$\mathcal{V}(N_c = 2, N_f^D = 1) = \mathcal{V}_g^{\text{np}}(N_c = 2, M, L; \{q\}) + \mathcal{V}_{\text{adj}}(N_c = 2, N_f^D = 1, L, m, \phi; \{q\}), \quad (2.33)$$

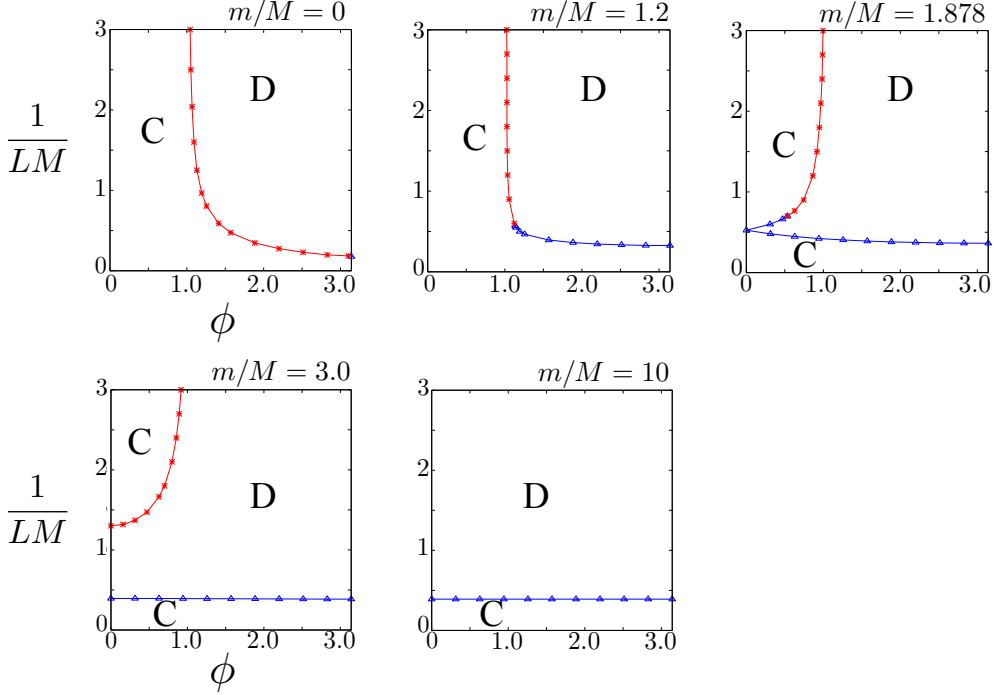


Figure 5. Phase diagrams for $N_c = 2$ and $N_f^D = 1$ with varying m/M . The blue line with triangles (\triangle) denotes a second-order phase transition, and the red line with asterisks ($*$) a first-order phase transition. Symbols C and D are defined as before. Spontaneous chiral symmetry breaking is not considered at this stage.

with \mathcal{V}_{adj} defined in (2.8). This extends our analysis for small L in Section 2.1 to the entire domain $0 < L < \infty$. Our main motivation here is two-fold: First, we aim to grasp how the center-changing transition at small L is related to the finite-temperature deconfinement transition at $L^{-1} = T_d$ and $\phi = \pi$; Secondly, we explore by changing m how the phase structure of massless QCD(adj) ($m = 0$) evolves into that of the pure Yang-Mills theory ($m = \infty$). Spontaneous breaking of chiral symmetry will be neglected for the moment; it is the main subject of Section 3.

In Figure 5 we present the numerically obtained phase diagrams on $1/L$ - ϕ space with varying m . At $m = 0$ (top left in Figure 5), the finite-temperature ($\phi = \pi$) phase transition is found to be second order and occurs at $L^{-1} = T_d^{N_f^D=1} \simeq 0.177M$. In comparison to $T_d^{\text{YM}} \simeq 0.390M$, the transition temperature has been reduced by a factor of 0.45 by inclusion of massless fermions. It is notable that the deconfinement phase transition seems to become *first order* as soon as ϕ is detuned from π . At $m = 0$ the confining phase at low temperature $\frac{1}{L} \ll M$ is continuously connected to the gauge-symmetry-broken phase at $\frac{1}{L} \gg M$. This is not a contradiction, because there is no gauge-invariant order parameter that characterizes the Higgs phenomenon. For $\frac{1}{L} \gg M$, the previous one-loop analysis is valid (recall (2.12)) and we expect the center-changing transition to occur at $\phi = 0.326\pi \simeq 1.024$ — indeed this is what we see in the figure.

As m is increased from zero, the second-order transition line emanating from the $\phi = \pi$ axis extends into the interior of the phase diagram. Passing through a tricritical point, it becomes first order.¹⁵ At $m/M \simeq 1.878$, the second-order line hits the $\phi = 0$ axis, and for larger m the confined phase is separated into two domains. As m is further increased, the confined (gauge-symmetry-broken) phase is pushed to higher and higher $\frac{1}{LM}$ and disappears from the figure; the phase diagram finally reduces to that of pure Yang-Mills theory, which is independent of ϕ . Such a change of the phase structure is consistent with the expected decoupling of fermions for $\frac{1}{L} \lesssim m$. If m is interpreted as mimicking the *constituent* quark mass, then an analog of the above behavior may well arise in the phase diagram of full-fledged QCD(adj) as well. In particular, the fact that heavy fermions cannot sustain the center-symmetric phase at intermediate L could be detrimental to the concept of “adiabatic continuity” from small L to large L [76–79] and to the large- N volume independence, so we will revisit this issue in Section 3.

Finally, in Figure 6, we depict the phase diagram of the same theory, but this time on the $(\frac{1}{LM}, \frac{m}{M})$ plane for a variety of ϕ . These figures clearly show how the phase structure changes with the boundary conditions. In the top left panel of Figure 6, the transition curve reaches its lowest point with $m/M = 1.878$, in agreement with the top right panel of Figure 5. Keeping track of the evolution of the phase diagram in Figure 6, one sees a qualitative global change of the phase diagram at $\phi \simeq 0.326\pi$, which is exactly the phase transition point in one-loop perturbation theory (cf. (2.12)). For ϕ greater than this value, even massless fermions cannot maintain a center-symmetric phase at large $\frac{1}{LM}$. Direct comparison of these model predictions and lattice simulations for $\phi = 0$ [37, 38] will be postponed to Section 3 where dynamical chiral symmetry breaking is taken into account.

A caveat is in order concerning the validity of the mean-field approximation we used.¹⁶ In effective models for QCD and pure Yang-Mills theory, it has been known that treating the Polyakov-loop matrix as a naive mean field is quite subtle and can even cause pathological behaviors [115]. For instance, the relation $\langle \text{Tr}_{\text{adj}} \Omega \rangle = |\langle \text{Tr} \Omega \rangle|^2 - 1$, valid in a naive mean-field approximation, is at variance with the lattice data where vanishingly small values are reported for both $\langle \text{Tr} \Omega \rangle$ and $\langle \text{Tr}_{\text{adj}} \Omega \rangle$ at $T < T_d$ [116]. Presumably one can expect this approximation to work accurately only under special circumstances, e.g., in the large- N limit and in the weak-coupling regime at small S^1 . Attempts to fix problems, e.g., through the use of Weiss mean-field approximation, are reported in the literature [11, 115, 117, 118]. It seems to be a very promising future direction to extend our work using such more refined approximation schemes.

3 Impact of chiral symmetry breaking

In this section we will incorporate the effect of dynamical chiral symmetry breaking to study the interplay of center and chiral symmetry on the phase diagram of QCD(adj). In Section 3.1 we review global symmetries of QCD(adj) and comment on restrictions on the possible

¹⁵A similar tricritical point has been found numerically in deformed Yang-Mills theory [114].

¹⁶This caveat also pertains to Section 3 where chiral and center symmetry breaking are simultaneously considered.

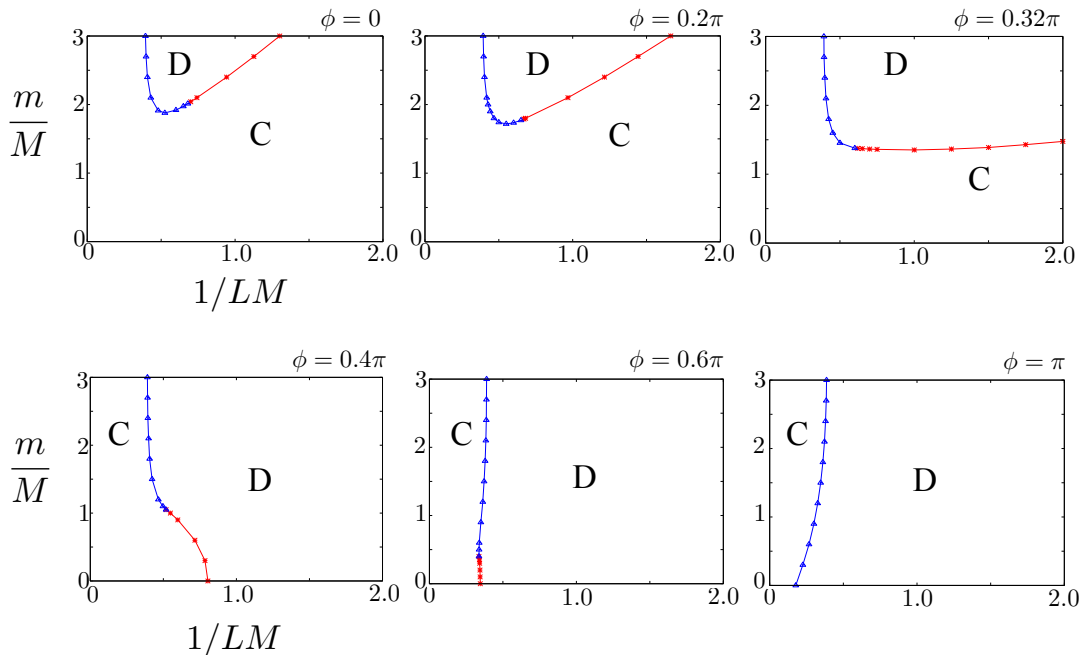


Figure 6. Phase diagram for $N_c = 2$ and $N_f^D = 1$ with $\phi \in \{0, 0.2\pi, 0.32\pi, 0.4\pi, 0.6\pi, \pi\}$. The blue line with triangles (\triangle) denotes a second-order phase transition, and the red line with asterisks ($*$) a first-order phase transition.

patterns of symmetry breaking. The insights obtained here are used for an appropriate model building in Section 3.2, where we analyze an NJL-type model with twisted boundary conditions using a high-temperature expansion. In Section 3.3 the PNJL model is solved numerically and its phase diagram is presented.

3.1 Chiral symmetry in QCD(adj)

In QCD(adj) on \mathbb{R}^4 in the chiral limit, the flavor symmetry of adjoint fermions is given by $U(1)_A \times SU(N_f^W)$ with $N_f^W = 2N_f^D$, which is larger than the standard symmetry $U(1)_A \times U(1)_B \times SU(N_f^D)_R \times SU(N_f^D)_L$ owing to the reality of the adjoint representation [6, 8].¹⁷ Instantons further break $U(1)_A$ down to $\mathbb{Z}_{2N_c N_f^W}$ explicitly, for the case of $SU(N_c)$ gauge theory [119]. The spontaneous breaking of continuous and discrete chiral symmetries can be probed by $\langle \text{Tr} \lambda^f \lambda^g \rangle$ and $\langle \det \text{Tr} \lambda^f \lambda^g \rangle$, respectively, where λ^f ($f = 1, \dots, N_f^W$) are adjoint Weyl fermions and ‘Tr’ denotes a trace over color indices. On small S^1 with PBC, $\mathbb{Z}_{2N_c N_f^W}$ is spontaneously broken to $\mathbb{Z}_{2N_f^W}$ yielding N_c degenerate vacua [44, 120].

Now we consider QCD(adj) on $\mathbb{R}^3 \times S^1$ with twisted boundary conditions ($0 \leq \phi \leq \pi$). Since imposing a twist ϕ on Dirac fermions Ψ as in (1.1) is equivalent to imposing a twist ϕ on half of the Weyl fermions and $-\phi$ on the other half, it follows that the flavor symmetry is *explicitly broken* by ϕ down to $U(1)_A \times U(1)_B \times SU(N_f^W/2)_R \times SU(N_f^W/2)_L$, except for $\phi/\pi \in \mathbb{Z}$ at which the full symmetry $U(1)_A \times SU(N_f^W)$ is recovered. This can also be seen

¹⁷We only consider even N_f^W (cf. Section 2.1).

as follows: a twist is equivalent to a constant background U(1) gauge field $A_4 = \phi/L$, which spoils the reality of the adjoint Dirac operator and reduces the flavor symmetry down to that of fermions in a complex representation. Since the enlarged symmetry is broken, it is more appropriate to use $\langle \text{Tr } \bar{\Psi} \Psi \rangle$ instead of $\langle \text{Tr } \lambda \lambda \rangle$ as an order parameter for flavor symmetry breaking.

A rough picture on the chiral phase structure is as follows. For $L \gg \Lambda_{\text{QCD}}^{-1}$, continuous chiral symmetry is spontaneously broken (for N_f^W outside the conformal window) for all $0 \leq \phi \leq \pi$. For $L \ll \Lambda_{\text{QCD}}^{-1}$, by contrast, the running coupling is small and chiral symmetry will be restored. Thus there must be a chiral transition at some $L = L_\chi(\phi)$ for any $0 \leq \phi \leq \pi$.

As asymptotic freedom requires $N_f^D < 11/4$ (see (2.1)), either $N_f^D = 1$ or 2 is possible. Let us discuss the two cases separately.

- $N_f^D = 1$: Non-anomalous global symmetry is $\frac{(\mathbb{Z}_{4N_c})_A \times \text{SU}(2)}{\mathbb{Z}_2}$ for $\phi = 0$ or π , and $\frac{(\mathbb{Z}_{4N_c})_A \times \text{U}(1)_B}{\mathbb{Z}_2}$ for $0 < \phi < \pi$.¹⁸ The thermal chiral transition at $\phi = \pi$, driven by $\langle \text{Tr } \bar{\Psi} \Psi \rangle \neq 0$, should be either first order, or second order in the O(3) universality class [121, 122].
- $N_f^D = 2$: Non-anomalous global symmetry is $\frac{(\mathbb{Z}_{8N_c})_A \times \text{SU}(4)}{\mathbb{Z}_4}$ for $\phi = 0$ or π , and $\frac{(\mathbb{Z}_{8N_c})_A \times \text{U}(1)_B \times \text{SU}(2)_R \times \text{SU}(2)_L}{\mathbb{Z}_4 \times (\mathbb{Z}_2)_{R+L}}$ for $0 < \phi < \pi$. The thermal chiral transition at $\phi = \pi$, driven by $\langle \text{Tr } \bar{\Psi} \Psi \rangle \neq 0$, is likely to be second order for $N_c = 3$ according to lattice data [3, 4], which should belong to the SU(4)/SO(4) universality class [121, 122].

As one can see above, $N_f^D = 1$ QCD(adj) is distinct from $N_f^D = 2$ in that the chiral condensate $\langle \text{Tr } \bar{\Psi} \Psi \rangle$ breaks no continuous symmetry at $\phi \neq 0$. We now argue that the pattern of *discrete* chiral symmetry breaking for $N_f^D = 1$ is dependent on the background holonomy through the existence of yet another condensate $\langle \det \text{Tr } \lambda^f \lambda^g \rangle$. The latter assumes a nonzero VEV if either of the following two conditions is met:

- (1) If $\langle \text{Tr } \bar{\Psi} \Psi \rangle$ is nonzero, it naturally induces a nonzero VEV of $\langle \det \text{Tr } \lambda^f \lambda^g \rangle$ because there is no symmetry that protects the latter from taking a nonzero value.
- (2) If the holonomy is center-symmetric, then instantons split into N_c constituent monopoles. The fermionic zero modes attached to each monopole contribute to making $\langle \det \text{Tr } \lambda^f \lambda^g \rangle$ nonzero [19, 20].¹⁹

¹⁸The common subgroup \mathbb{Z}_2 is factored out to avoid double counting of symmetries. Same for $N_f^D = 2$.

¹⁹Although this picture is justified only in a small- L semiclassical domain, we suspect that the determinantal condensate is generally supported by a nontrivial holonomy. Indeed, a recent preprint [123] reports that $\langle \lambda \lambda \rangle$ in SYM goes to zero at approximately the same temperature as the deconfinement transition, which corroborates our point of view.

The above consideration suggests that, at $\phi \neq 0$, we should take into account the background Polyakov loop to figure out the correct universality class of the chiral transition driven by $\langle \text{Tr } \bar{\Psi} \Psi \rangle$.

- In a center-symmetric phase with $\langle P_F \rangle = 0$, the axial symmetry $(\mathbb{Z}_{4N_c})_A$ is spontaneously broken to \mathbb{Z}_4 through $\langle \det \text{Tr } \lambda^f \lambda^g \rangle \neq 0$. Therefore $\langle \text{Tr } \bar{\Psi} \Psi \rangle$ serves as an order parameter of the symmetry breaking $\mathbb{Z}_4 \rightarrow \mathbb{Z}_2$. The chiral transition, if continuous, will belong to the 3d Ising universality class.
- In a deconfined phase with $\langle P_F \rangle \neq 0$, $\langle \det \text{Tr } \lambda^f \lambda^g \rangle$ will go to zero simultaneously with $\langle \text{Tr } \bar{\Psi} \Psi \rangle$ at the chiral transition. Therefore the pattern is $\mathbb{Z}_{4N_c} \rightarrow \mathbb{Z}_2$. The chiral transition, if continuous, will belong to the same universality class as spin systems in 3d with \mathbb{Z}_{2N_c} symmetry breaking.

This issue will be taken up again in Section 3.3 when we discuss the phase diagram of QCD(adj).

A comment is in order concerning the $U(1)_B$ baryon number symmetry. As is well known, QCD(adj) enters a superfluid phase with diquark condensate $\langle \text{Tr } \Psi \Psi \rangle \neq 0$ for high *real* chemical potential [6, 10]. However, it does not occur for *imaginary* chemical potential (i.e., $\phi \neq 0$) because it is forbidden by the Vafa-Witten theorem [124] for any nonzero bare mass m . The argument goes as follows. If $U(1)_B$ were spontaneously broken, there will be a massless NG mode $M \sim \Psi \Psi$, whose correlator $\langle M(x) M^\dagger(y) \rangle$ decays more slowly than exponentially at large $|x - y|$. On the other hand, (i) if the path-integral measure is positive definite, and (ii) if the Dirac operator is anti-hermitian, one can prove that the fermion propagator $S(x, y)$ in an arbitrary gauge field background decays at least as fast as $e^{-m|x-y|}$ at large distances [124]. Thus $|\langle M(x) M^\dagger(y) \rangle| \propto |S(x, y)|^2 \leq e^{-2m|x-y|}$, which contradicts the existence of a massless NG mode in this channel. As the conditions (i) and (ii) are both satisfied for QCD(adj) at any ϕ , we conclude that $U(1)_B$ is not spontaneously broken, and $\langle \text{Tr } \Psi \Psi \rangle = 0$. This argument equally applies to both $N_f^D = 1$ and 2. For $N_f^D = 2$, $\langle \text{Tr } \Psi \Psi \rangle = 0$ can also be proven by means of QCD inequalities [125–127].

Thus the diquark condensate vanishes in QCD(adj) for any ϕ , as long as $m \neq 0$. If we define the chiral limit as $m \rightarrow +0$, this conclusion should remain valid in the chiral limit as well.²⁰ This allows us to take $\langle \text{Tr } \bar{\Psi} \Psi \rangle$ as the primary order parameter of flavor symmetry breaking in QCD(adj) within the analysis of the phase diagram.

3.2 PNJL model: an analytical study

In this subsection we study the ϕ -dependence of dynamical chiral symmetry breaking analytically. For simplicity, the bare mass of fermions is set to zero.

From here on, we shall concentrate on the $N_f^D = 1$ case, for the sake of simplicity and to evade the conformal window. We want to investigate chiral symmetry realization for general ϕ using an effective model. For this purpose, it is essential that the model reflects

²⁰Note that there are other ways to approach the chiral limit; for example, in the presence of a diquark source $j \Psi \Psi$, the ground state may depend on which of the limits $m \rightarrow 0$ and $j \rightarrow 0$ were taken first [6, 10]. The arguments presented above do not apply to the case with $j \neq 0$.

the special symmetries of QCD(adj) correctly.²¹ The form of four-fermion interaction that respects $SU(2N_f^D)$ symmetry of QCD(adj) has been determined in Ref. [11]. For $N_f^D = 1$, two kinds of interaction have been identified:

$$\mathcal{L}_{U(2)} = \frac{G}{2} [(\bar{\Psi}\Psi)^2 + (\bar{\Psi}i\gamma_5\Psi)^2 + |\bar{\Psi}^C\gamma_5\Psi|^2 + |\bar{\Psi}^C\Psi|^2] \quad (3.1a)$$

$$\mathcal{L}_{SU(2)} = \frac{G}{2} [(\bar{\Psi}\Psi)^2 - (\bar{\Psi}i\gamma_5\Psi)^2 + |\bar{\Psi}^C\gamma_5\Psi|^2 - |\bar{\Psi}^C\Psi|^2] \quad (3.1b)$$

where G is a coupling constant of dimension $[\text{mass}]^{-2}$, Ψ is the adjoint Dirac spinor, $\Psi^C \equiv C\bar{\Psi}^T$ is the charge-conjugated spinor, and the color indices are assumed to be properly contracted. Both (3.1a) and (3.1b) entertain $SU(2)$ symmetry and, for $0 < \phi < \pi$, break it down to $U(1)_B$ explicitly, in agreement with the expectation for QCD(adj). Their difference is that, as the notation suggests, $\mathcal{L}_{U(2)}$ is invariant under $U(1)_A$ whereas $\mathcal{L}_{SU(2)}$ is not; the latter breaks $U(1)_A$ down to \mathbb{Z}_4 . On the other hand, the correct unbroken axial symmetry for $N_f^D = 1$ is \mathbb{Z}_{4N_c} , as remarked above. This means neither $\mathcal{L}_{U(2)}$ nor $\mathcal{L}_{SU(2)}$ has the correct axial symmetry. Is it important for us? Probably yes, because the axial anomaly can change the order of the chiral phase transition, and in case of continuous transition, can change the corresponding universality class, as revealed in the renormalization group analysis [121, 122, 128]. However, such a detailed description of the chiral transition is beyond the scope of this paper. Instead, in what follows, we will just be satisfied with demonstrating the chiral phase structure on $L^{-1-\phi}$ plane. For practical calculations we would like to use a linear combination of $\mathcal{L}_{U(2)}$ and $\mathcal{L}_{SU(2)}$ in order to mimic the effect of anomaly. Namely, we consider a chiral effective model whose fermionic part is given by

$$\mathcal{L}_{N_f^D=1} = \text{Tr}[\bar{\Psi}D_{\text{adj}}\Psi] + \frac{1}{2}(\mathcal{L}_{U(2)} + \mathcal{L}_{SU(2)}) \quad (3.2)$$

$$= \text{Tr}[\bar{\Psi}D_{\text{adj}}\Psi] + \frac{G}{2} [(\bar{\Psi}\Psi)^2 + |\bar{\Psi}^C\gamma_5\Psi|^2], \quad (3.3)$$

where $D_{\text{adj}}\Psi \equiv \gamma_\mu(\partial_\mu\Psi + i[A_\mu, \Psi])$ and $A_\mu = \delta_{\mu 4}A_4$ with A_4 given in (2.3). The bare mass is set to zero. This is a variant of the so-called PNJL model [84]. In the following, we treat the gauge sector along the lines of Section 2.2 using the phenomenological gluonic potential $\mathcal{V}_g^{\text{np}}$. If the coupling G is zero, we are brought back to the model of Section 2.2, whose total effective potential is already given in (2.33) for the case of $N_c = 2$. In Appendix B, the present model is juxtaposed with other chiral effective models in the literature for completeness.

Now, we switch on $G > 0$ and investigate its impact on the phase diagram. The model (3.3) can be solved in the mean-field approximation following a standard procedure [129, 130]. From Section 3.1, we expect $\langle \text{Tr} \bar{\Psi}^C \gamma_5 \Psi \rangle = 0$ in QCD(adj), and will assume this in the current effective model as well. Then the total thermodynamic potential at the

²¹This point was not stressed in earlier works [80, 112]; see Appendix B for a detailed comparison of chiral models in the literature.

mean-field level reads²²

$$\begin{aligned} \mathcal{V}_{\text{tot}}(N_c, N_f^D = 1, \phi, L, m_{\text{dyn}}; \{q\}) \\ = \mathcal{V}_{\text{g}}^{\text{np}}(N_c, M, L; \{q\}) + \mathcal{V}_{\text{adj}}(N_c, N_f^D = 1, L, m_{\text{dyn}}, \phi; \{q\}) + \mathcal{V}_{\chi}(N_c, G, \Lambda_{\text{UV}}, m_{\text{dyn}}), \end{aligned} \quad (3.4)$$

where $m_{\text{dyn}} \equiv -G\langle\text{Tr}\bar{\Psi}\Psi\rangle$ is the dynamical mass of fermions, $\mathcal{V}_{\text{g}}^{\text{np}}$ and \mathcal{V}_{adj} are defined in (2.32) and (2.8), respectively, and

$$\begin{aligned} \mathcal{V}_{\chi}(N_c, G, \Lambda_{\text{UV}}, m_{\text{dyn}}) &= \frac{m_{\text{dyn}}^2}{2G} - 2(N_c^2 - 1) \int_{|p| < \Lambda_{\text{UV}}} \frac{d^3p}{(2\pi)^3} \sqrt{p^2 + m_{\text{dyn}}^2} \\ &= \frac{m_{\text{dyn}}^2}{2G} - \frac{N_c^2 - 1}{8\pi^2} \left\{ \Lambda_{\text{UV}}(m_{\text{dyn}}^2 + 2\Lambda_{\text{UV}}^2) \sqrt{m_{\text{dyn}}^2 + \Lambda_{\text{UV}}^2} \right. \\ &\quad \left. + m_{\text{dyn}}^4 \log \frac{m_{\text{dyn}}}{\Lambda_{\text{UV}} + \sqrt{m_{\text{dyn}}^2 + \Lambda_{\text{UV}}^2}} \right\}, \end{aligned} \quad (3.5)$$

$$(3.6)$$

where Λ_{UV} is a momentum cutoff.

Finding the minimum of $\mathcal{V}_{\text{tot}}(N_c, N_f^D = 1, \phi, L, m_{\text{dyn}}; \{q\})$ for all $0 \leq \phi \leq \pi$ requires tedious numerics, which will be done in Section 3.3 for the simplest case of $N_c = 2$. Before that, let us try to capture qualitative features of the chiral transition for varying ϕ by analytical means, which proves helpful in developing an intuitive picture for the interplay of confinement and chiral symmetry breaking. To facilitate practical calculations, we “freeze” the dynamics of the gauge sector by fixing a particular holonomy and then solve the chiral dynamics in this background.²³ Section 3.2.1 deals with the case of a trivial holonomy $\Omega = \mathbb{1}$ where the model reduces to the classical NJL model but with a twisted boundary condition. In Section 3.2.2 we turn to the case of a center-symmetric holonomy.

3.2.1 Trivial holonomy

Assuming a continuous chiral phase transition, m_{dyn} is small in the vicinity of chiral restoration, and the effective potential can be expanded in terms of m_{dyn} . With inspection we get

$$\mathcal{V}_{\chi}(N_c, G, \Lambda_{\text{UV}}, m_{\text{dyn}}) = \text{const.} + \left(\frac{1}{2G} - \frac{N_c^2 - 1}{4\pi^2} \Lambda_{\text{UV}}^2 \right) m_{\text{dyn}}^2 + O(m_{\text{dyn}}^4). \quad (3.7)$$

In the decompactification limit $L \rightarrow \infty$, \mathcal{V}_{adj} in (3.4) drops off and \mathcal{V}_{χ} solely determines the chiral symmetry realization. Since we are interested in theories in which chiral symmetry

²²At the mean-field level, the thermodynamic potential does not depend on whether we have included the diquark channel in the four-fermi interaction or not. This is simply because we have no diquark condensate in the present situation. However, once we go beyond the mean-field approximation and incorporate mesonic fluctuations, it matters to have the four-fermion interaction (3.3) with the correct symmetry of QCD(adj).

²³This can be implemented in actual lattice simulations with the aid of double-trace deformations [59].

is broken on \mathbb{R}^4 , the coefficient of the second-order term should be negative, i.e.,²⁴

$$G > \frac{2\pi^2}{N_c^2 - 1} \frac{1}{\Lambda_{\text{UV}}^2}. \quad (3.8)$$

At finite L , \mathcal{V}_{adj} gives a nonzero contribution. Putting $\Omega = \mathbb{1}$ in (2.7), one finds

$$\mathcal{V}_{\text{adj}}(N_c, N_f^D = 1, L, m_{\text{dyn}}, \phi; \{q\}) = (N_c^2 - 1) \frac{m_{\text{dyn}}^2}{\pi^2 L^2} \sum_{n=1}^{\infty} \left(\frac{K_2(nLm_{\text{dyn}})}{n^2} e^{in\phi} + \text{c.c.} \right). \quad (3.9)$$

A naive expansion of K_2 in powers of m_{dyn} fails, because the sum over n becomes termwise divergent. The correct expansion in m_{dyn} for generic ϕ has been derived quite recently by Klajn [131]. Using formulas from Ref. [131], we obtain

$$\begin{aligned} \mathcal{V}_{\text{adj}}(N_c, N_f^D = 1, L, m_{\text{dyn}}, \phi; \{q\}) = & - (N_c^2 - 1) \left[\frac{4\pi^2}{3L^4} B_4 \left(\left\| \frac{\phi}{2\pi} \right\| \right) + \frac{1}{L^2} B_2 \left(\left\| \frac{\phi}{2\pi} \right\| \right) m_{\text{dyn}}^2 \right] \\ & + \{ \text{higher orders in } m_{\text{dyn}} \}, \end{aligned} \quad (3.10)$$

where $B_2(x)$ and $B_4(x)$ are the Bernoulli polynomials and $\|x\| \equiv x - [x] \in [0, 1)$ is the fractional part of x .²⁵

Combining (3.7) and (3.10), we arrive at the expansion of the total potential:

$$\begin{aligned} \mathcal{V}_{\text{tot}}(N_c, N_f^D = 1, \phi, L, m_{\text{dyn}}; \{q\}) \Big|_{O(m_{\text{dyn}}^2)} \\ = \left[\frac{1}{2G} - \frac{N_c^2 - 1}{4\pi^2} \Lambda_{\text{UV}}^2 - \frac{N_c^2 - 1}{L^2} B_2 \left(\left\| \frac{\phi}{2\pi} \right\| \right) \right] m_{\text{dyn}}^2. \end{aligned} \quad (3.11)$$

We mention that this expression has been independently derived by Benić [132].

As $B_2(x) = x^2 - x + 1/6$ changes sign at $x = (3 \pm \sqrt{3})/6$, it is useful to divide $0 \leq \phi \leq \pi$ into two intervals.

- $(1 - \frac{1}{\sqrt{3}})\pi < \phi \leq \pi$: $B_2(\frac{\phi}{2\pi}) < 0$. For sufficiently small L , chiral symmetry is restored. The chiral transition line on L^{-1} - ϕ plane is given by

$$\frac{1}{\Lambda_{\text{UV}} L} = \sqrt{\left| B_2 \left(\frac{\phi}{2\pi} \right) \right|^{-1} \left(\frac{1}{4\pi^2} - \frac{1}{2(N_c^2 - 1)G\Lambda_{\text{UV}}^2} \right)}, \quad (3.12)$$

which up to typos confirms the result of Ref. [132, eq. (6)].

- $0 \leq \phi \leq (1 - \frac{1}{\sqrt{3}})\pi$: $B_2(\frac{\phi}{2\pi}) \geq 0$. Chiral symmetry is spontaneously broken at all circumferences, $0 < L < \infty$. It is intriguing that the threshold $\phi = (1 - \frac{1}{\sqrt{3}})\pi \simeq 0.42\pi$ is a pure number, independent of any parameter of the model.

²⁴Chiral symmetry in this model would be unbroken on \mathbb{R}^4 if (3.8) is not satisfied. Although such a chirally-symmetric phase is reminiscent of the IR conformal phase of QCD with many flavors, care must be taken, because the conformality is broken by the dimensionful parameter G *explicitly*, and also because the pointlike four-fermion interaction of the NJL model is presumably a poor approximation to the long-range interaction in the conformal phase of QCD mediated by massless gluons.

²⁵The leading higher-order term in (3.10) is $O(m_{\text{dyn}}^4 \log m_{\text{dyn}}^2)$ for $\phi \neq 0$ and $O(|m_{\text{dyn}}|^3)$ for $\phi = 0$ [131].

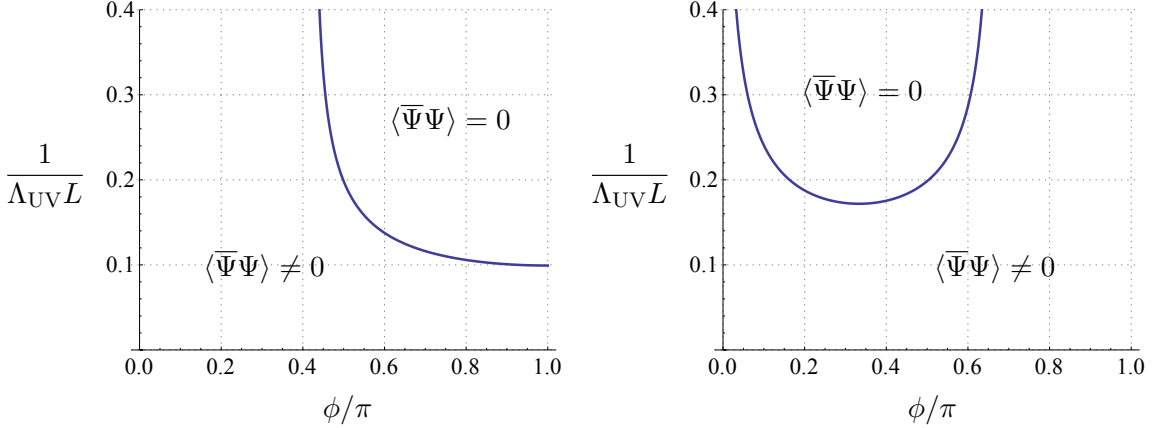


Figure 7. Phase structures of the NJL model for trivial holonomy (**left**) and for center-symmetric holonomy (**right**) are juxtaposed for $N_c = 2$, $N_f^D = 1$ and $G\Lambda_{\text{UV}}^2 = 6.8$. In both figures, the phase transition is second order.

In Figure 7 (left) we show the $N_c = 2$ phase structure with the parameter choice of $G\Lambda_{\text{UV}}^2 = 6.8$ that satisfies the bound (3.8). The region with larger $\frac{1}{\Lambda_{\text{UV}}L}$ is not shown because the model would be less reliable there owing to cutoff artifacts.²⁶ The tendency that the chiral transition moves to higher L^{-1} for smaller ϕ is clearly visible in the figure, which occurs *within* the domain of validity of the model ($L^{-1} \lesssim \Lambda_{\text{UV}}$). A simplistic way of explaining this is to posit that a smaller ϕ which decreases the lowest Matsubara frequency (ϕ/L) of fermions would facilitate symmetry breaking at low energy. We expect that the same behavior will be seen in actual QCD(adj), in a phase with trivial holonomy.

3.2.2 Center-symmetric holonomy

Next, we consider a center-symmetric background field

$$A_4 = \frac{1}{L} \text{diag} \left(\left(-1 + \frac{1}{N_c} \right) \pi, \left(-1 + \frac{3}{N_c} \right) \pi, \dots, \left(1 - \frac{1}{N_c} \right) \pi \right). \quad (3.13)$$

The eigenvalues of $\Omega = e^{iA_4}$ are equally spaced on a unit circle as depicted in Figure 8. It is easy to check that

$$\text{Tr}_{\text{adj}}(\Omega^n) = |\text{Tr}(\Omega^n)|^2 - 1 = \begin{cases} N_c^2 - 1 & \text{for } n \equiv 0 \pmod{N_c} \\ -1 & \text{otherwise} \end{cases}. \quad (3.14)$$

Using this property in (2.7), we obtain

$$\mathcal{V}_{\text{adj}}(N_c, N_f^D = 1, L, m_{\text{dyn}}, \phi; \{q\}) = \frac{m_{\text{dyn}}^2}{\pi^2 L^2} \sum_{n=1}^{\infty} \frac{K_2(nLm_{\text{dyn}})}{n^2} e^{in\phi} (N_c^2 \delta_{n,0}^{(\text{mod } N_c)} - 1) + \text{c.c.}, \quad (3.15)$$

²⁶The absence of chiral restoration for $0 \leq \phi \leq (1 - \frac{1}{\sqrt{3}})\pi$ is presumably a model artifact and not a genuine property of QCD(adj) because the gauge coupling runs to zero at $L\Lambda_{\text{QCD}} \ll 1$ and a spontaneous symmetry breaking should be hindered. This idea is consistent with the observation that a divergence of T_c also occurs in a non-relativistic effective model with a cutoff [133] whereas it does not occur in the renormalizable Gross-Neveu model in 2 dimensions [29], with twisted boundary conditions, respectively.

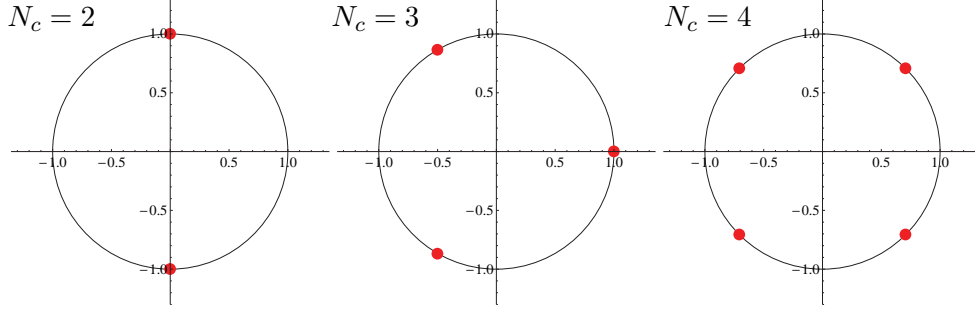


Figure 8. Eigenvalues of a center-symmetric holonomy Ω for $N_c = 2, 3$ and 4 represented as red blobs on a unit circle in the complex plane.

with $\delta_{n,0}^{(\text{mod } N_c)} = 1$ for $n \equiv 0 \pmod{N_c}$ and $= 0$ otherwise. With the aid of the identity

$$\delta_{n,0}^{(\text{mod } N_c)} = \frac{1}{N_c} \sum_{k=0}^{N_c-1} e^{in\frac{2\pi k}{N_c}}, \quad (3.16)$$

(3.15) can be cast into the form

$$\begin{aligned} \mathcal{V}_{\text{adj}}(N_c, N_f^D = 1, L, m_{\text{dyn}}, \phi; \{q\}) = & N_c \sum_{k=0}^{N_c-1} \left\{ \frac{m_{\text{dyn}}^2}{\pi^2 L^2} \sum_{n=1}^{\infty} \frac{K_2(nLm_{\text{dyn}})}{n^2} e^{in\left(\phi + \frac{2\pi k}{N_c}\right)} + \text{c.c.} \right\} \\ & - \left\{ \frac{m_{\text{dyn}}^2}{\pi^2 L^2} \sum_{n=1}^{\infty} \frac{K_2(nLm_{\text{dyn}})}{n^2} e^{in\phi} + \text{c.c.} \right\}. \end{aligned} \quad (3.17)$$

The expansion in terms of m_{dyn} readily follows from (3.10). Combined with (3.7) it yields

$$\mathcal{V}_{\text{tot}}(N_c, N_f^D = 1, \phi, L, m_{\text{dyn}}; \{q\}) \Big|_{\mathcal{O}(m_{\text{dyn}}^2)} = \left[\frac{1}{2G} - \frac{N_c^2 - 1}{4\pi^2} \Lambda_{\text{UV}}^2 + \frac{1}{L^2} \xi\left(N_c; \frac{\phi}{2\pi}\right) \right] m_{\text{dyn}}^2, \quad (3.18)$$

with

$$\xi(N_c; x) \equiv B_2(\|x\|) - N_c \sum_{k=0}^{N_c-1} B_2\left(\left\|x + \frac{k}{N_c}\right\|\right). \quad (3.19)$$

The behavior of $\xi(N_c; x)$ depends on N_c . For $N_c = 2$, it crosses zero at $x = k/3$ for $k \in \mathbb{Z}$.

- $0 < \phi < 2\pi/3$: $\xi(N_c; x) > 0$. For sufficiently small L , chiral symmetry is restored. The critical line is given by

$$\frac{1}{\Lambda_{\text{UV}} L} = \sqrt{\xi\left(N_c; \frac{\phi}{2\pi}\right)^{-1} \left(\frac{N_c^2 - 1}{4\pi^2} - \frac{1}{2G\Lambda_{\text{UV}}^2}\right)}. \quad (3.20)$$

- $2\pi/3 \leq \phi \leq \pi$: $\xi(N_c; x) \leq 0$. Chiral symmetry is always broken for $0 < L < \infty$.

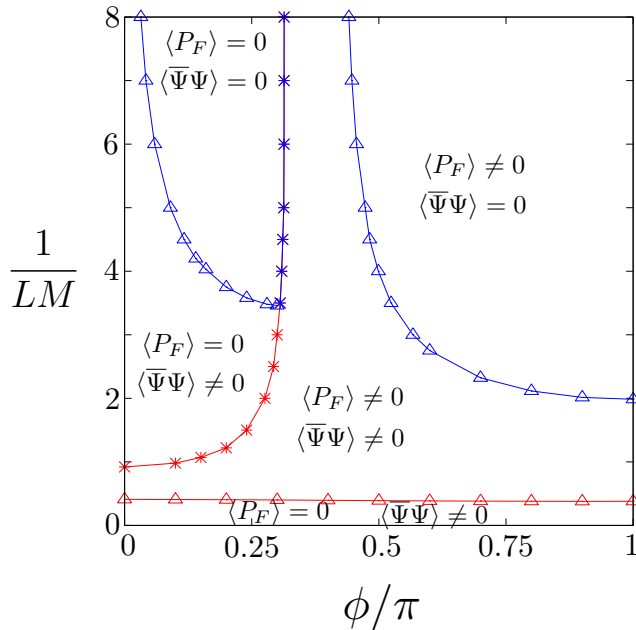


Figure 9. A numerically obtained phase diagram of the PNJL model for $N_c = 2$ and $N_f^D = 1$ in the mean-field approximation. The blue (red) line denotes chiral (deconfinement) transition, respectively. The triangles (Δ) represent a second-order transition and the asterisks ($*$) a first-order transition. The chiral and deconfinement transitions are degenerate for $\phi/\pi \simeq 0.3$ and $1/LM \gtrsim 3.4$. We note that chiral condensate also jumps from nonzero to another nonzero value at the first-order deconfinement transition (cf. Figure 11).

In Figure 7 (right) we show the $N_c = 2$ phase structure with the parameter choice $G\Lambda_{UV}^2 = 6.8$ again. In comparison to the case with trivial holonomy, the locus of the chirally symmetric phase is now drastically different; it has been shifted to smaller ϕ . The overall structure of the plots in Figure 7 are independent of the specific value of $G\Lambda_{UV}^2$ as long as the condition (3.8) is satisfied. We conclude that the coupling to the Polyakov loop plays an essential role for the chiral symmetry realization with twisted boundary conditions.

In Section 3.3 we will treat the holonomy as a dynamical variable and compare the analytical predictions with numerical results.

3.3 PNJL model: numerical results

We limit ourselves to $N_c = 2$ and $N_f^D = 1$ in the chiral limit $m = 0$ to make numerical computations easier. The model has three dimensionful parameters: M , G and Λ_{UV} . As we lack inputs from lattice simulations, there is no unique way to fix these parameters. In this study we will try two choices, so that by comparison one can see the parameter dependence of model predictions. As the first set of parameters, we use

$$G\Lambda_{UV}^2 = 6.8 \quad \text{and} \quad \Lambda_{UV} = 20M. \quad (3.21)$$

We note that $G\Lambda_{UV}^2$ in (3.21) is the same as used for Figure 7.

The phase diagram obtained from minimization of the thermodynamic potential (3.4) for $0 \leq 1/L \leq 8M$ and $0 \leq \phi \leq \pi$ is displayed in Figure 9. It has some notable features:

- The center phase structure at $1/LM \gg 1$ agrees with the one-loop analysis in (2.12), including a center-changing transition at $\phi = 0.326\pi$.
- At $\phi = \pi$, the chiral and deconfinement transitions occur at widely separated temperatures: we find $T_\chi \simeq 5T_d$, which is roughly consistent with the interpolation of lattice data for $N_f^D = 1/2$ and 2 in Ref. [2]. This is comparable to QCD(adj) with $N_c = 3$ and $N_f^D = 2$ where $T_\chi \simeq 8T_d$ [3, 4].
- The whole center phase structure of Figure 9 is well captured by Figure 5 with $m/M = 3.0$ which is the *bare* mass of fermions. This qualitative agreement is quite natural, given that the *dynamical* mass in the present setup, $m_{\text{dyn}} \simeq 0.12\Lambda_{\text{UV}} = 2.4M$ at $1/LM = 0$, is close to the value above. The opening of a deconfined window for $0.5 \lesssim \frac{1}{LM} \lesssim 1$ at $\phi = 0$ in Figure 9 may be interpreted as follows: the adjoint fermions with PBC, which favor a center-symmetric phase, are suppressed by their large (bare or dynamical) mass and fail to prevent the appearance of a center-broken phase at intermediate L .²⁷ This phenomenon was observed for $N_c = 3$ in lattice simulations at $\phi = 0$ [37, 38] and confirmed in model calculation [80]. Moreover, Figure 9 also reveals that the deconfined phase extends to $0 < \phi < \pi$ and separates the confining phase at small $1/L$ from that at large $1/L$ altogether, in the entire phase diagram. This is a new result of this work.
- The lines of chiral phase transition in Figure 9 are well described by the analytic curves from the high-temperature expansion (Figure 7). A notable difference, however, is that part of the critical line for center-symmetric holonomy (Figure 7, right) is excised in Figure 9 by a first-order deconfinement transition line. This is a manifestation of a nontrivial interplay between chiral and center symmetry.
- Chiral symmetry is broken at all $0 < L < \infty$ for $\phi = 0$ and $0.326\pi \leq \phi \leq (1 - \frac{1}{\sqrt{3}})\pi$. Actually, the fact that chiral symmetry is broken at $\phi = 0$ up to a much smaller L than at $\phi = \pi$ has been known from lattice simulation [37] and model calculations [80, 112, 134], whereas the behavior for $0.326\pi \leq \phi \leq (1 - \frac{1}{\sqrt{3}})\pi$ is a new finding here. Although the model seems to capture the actual tendency of QCD(adj), it has an intrinsic cutoff Λ_{UV} and may not be trusted at $1/L \gtrsim \Lambda_{\text{UV}}$; indeed, Ünsal showed that chiral symmetry at $\phi = 0$ is restored at sufficiently small L [43, 44].

In Figures 10 and 11 we display the expectation values of the chiral condensate and the Polyakov loop as a function of ϕ and L . The result shows that the first-order transition in $\langle P_F \rangle$ is quite strong and is accompanied by a finite jump in the chiral condensate.

As suggested by Figures 5 and 6, it is the magnitude of m_{dyn} at low $1/LM$ that effectively determines the presence or absence of the deconfined phase on the $\phi = 0$ axis.²⁸

²⁷At this point the reader may wonder why $N_f^W = 1$ adjoint fermion (called gluino) in $\mathcal{N} = 1$ SYM can sustain a center-symmetric phase at all L despite that $N_f^W = 2$ (> 1) adjoint fermions cannot. It could be explained if the dynamical mass of gluinos in SYM were much smaller than the dynamical mass originating from continuous chiral symmetry breaking for $N_f^W = 2$. This point deserves further study.

²⁸ m_{dyn} is roughly constant for $0 \leq 1/L \lesssim 2M$ as shown in Figure 11 (left).

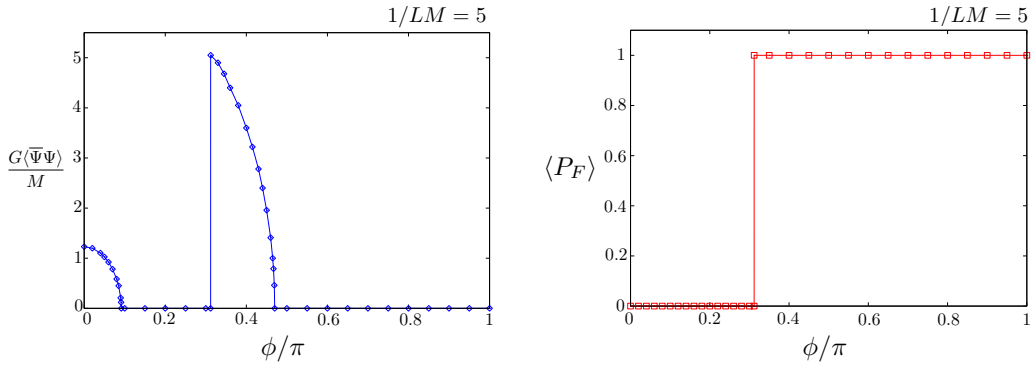


Figure 10. The ϕ -dependence of the chiral condensate (**left**) and the Polyakov loop in the fundamental representation (**right**) at $1/LM = 5$.

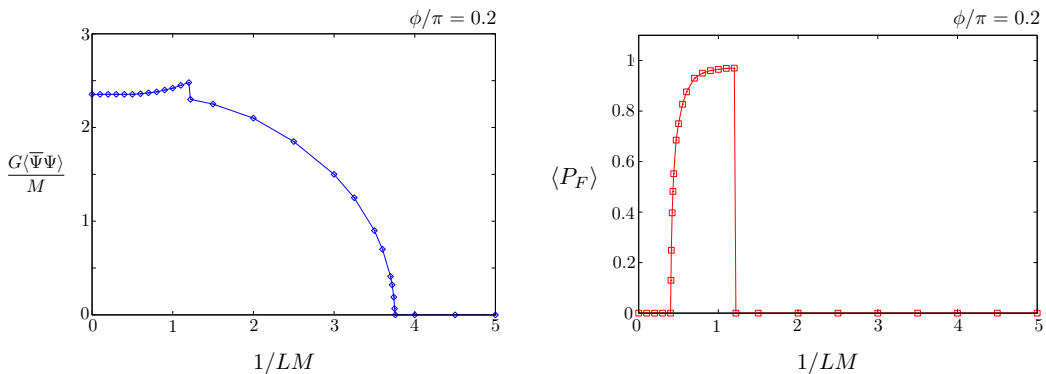


Figure 11. The L -dependence of the chiral condensate (**left**) and the Polyakov loop in the fundamental representation (**right**) at $\phi/\pi = 0.2$.

In Figure 9 the latter appears, because $m_{\text{dyn}} = 2.4M$ resulting from the parameter set (3.21) is greater than the threshold value, $1.878M$ (cf. Figure 5). Since the parameter fixing in the model is not unique, it is natural to ask whether the topology of the phase diagram could be altered or not with a different set of parameters. To address this issue, we also computed the phase diagram using the second set of parameters

$$G\Lambda_{\text{UV}}^2 = 6.8 \quad \text{and} \quad \Lambda_{\text{UV}} = 15M, \quad (3.22)$$

leading to $m_{\text{dyn}} = 1.77M$, which is reduced from the previous case by 25%. We note that $G\Lambda_{\text{UV}}^2$ in (3.22) is not changed from (3.21). For the transition temperatures at $\phi = \pi$, we found $T_\chi \simeq 4.5T_d$. The resulting phase diagram is presented in Figure 12 (right), in comparison with that of the previous parameter set (left). We only show the region with $1/LM \leq 2$ because there is no qualitative difference between the two diagrams in the rest of the phase diagram.

An important characteristic of Figure 12 (right) is that the conventional confining phase on \mathbb{R}^4 is now continuously connected to the other confining phase at large $1/LM$ where the gauge symmetry is spontaneously broken via the Hosotani mechanism. This is expected from Figures 5 and 6 since the dynamical mass here is lighter than the threshold value,

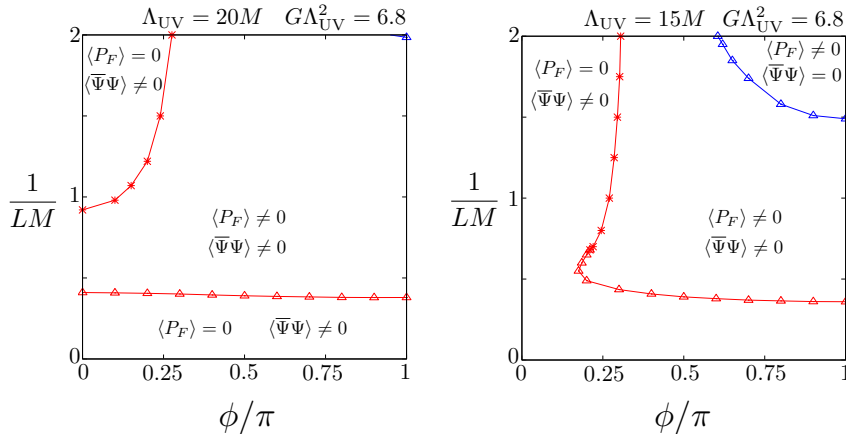


Figure 12. Phase diagrams of the PNJL model for $N_c = 2$ and $N_f^D = 1$ with two different parameter sets, (3.21) (left) and (3.22) (right), respectively. The triangles (Δ) represent a second-order transition and the asterisks ($*$) a first-order transition. The two confining phases are separated in the left diagram while it is connected in the right diagram.

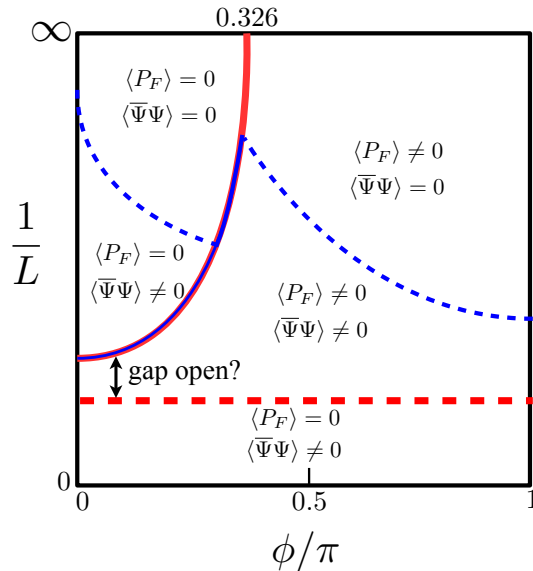


Figure 13. A conjectural phase diagram of QCD(adj) with $N_c = 2$ and $N_f^D = 1$. The red solid (dashed) line denotes a first-order (second-order) deconfinement transition. The blue solid (dashed) line denotes a first-order (second-order) chiral transition.

i.e., $m_{\text{dyn}} = 1.77M < 1.878M$. The fact that the global topology of the phase diagram can be altered with such a small change of parameters ($\Lambda_{UV} = 15M$ vs. $\Lambda_{UV} = 20M$) seems to highlight the crucial role of a delicate balance between dynamical mass m_{dyn} and the Yang-Mills scale M .

Finally, in Figure 13 we show our conjecture for the phase diagram of QCD(adj) which is based on all insights from the model. The absence of chiral restoration for certain ϕ in the PNJL model is remedied by hand. The interesting prediction here is the merger of chiral and deconfinement transitions, indicated by a thin blue line overlaid on a red line

in Figure 13. As for the center symmetry breaking at $\phi = 0$, at present we do not know which phase diagram of Figure 12 is the right one in QCD(adj), so we have indicated our ignorance by the annotation “gap open?” in Figure 13. Comparing our conjectural phase diagram with an early conjecture by Shuryak [75], we see several qualitative differences. Firstly, the lines of chiral and deconfinement transitions are assumed to intersect at a single point in Ref. [75], whereas our model calculation strongly suggests that they have an overlapping segment. Secondly, center symmetry at $\phi = 0$ is assumed to be unbroken for all $0 < L < \infty$ in Ref. [75], while this may not be necessarily true if the large constituent fermion mass is taken into account, as indicated in Figure 13.

The second-order chiral phase transition, represented by blue dashed lines in Figure 13, characterizes the breaking/restoration of *discrete* axial symmetry. On the basis of the arguments in Section 3.1, we expect that the chiral transitions on the right/left of the first-order deconfinement transition (red solid line in Figure 13) will exhibit different universal behaviors: on the left side, it should belong to the 3d Ising universality class, while on the right side, to the 3d spin systems with \mathbb{Z}_4 symmetry breaking.

We hope that these predictions in this paper will be tested in future lattice QCD simulations.

4 Summary and discussion

In this paper, we investigate QCD with adjoint fermions [QCD(adj)] on $\mathbb{R}^3 \times S^1$. In the past, QCD(adj) on $\mathbb{R}^3 \times S^1$ with the thermal boundary condition has been simulated on the lattice to test relationship between chiral symmetry breaking and confinement. QCD(adj) with the periodic boundary condition on S^1 has also been studied in the context of gauge symmetry breaking (the Hosotani mechanism [42]) and the semiclassical confinement due to bion condensation à la Ünsal [44]. However the other boundary conditions have not been systematically explored. In this work, we fill the gap by studying the non-perturbative dynamics of QCD(adj) on $\mathbb{R}^3 \times S^1$ with a generic boundary condition $0 \leq \phi \leq \pi$ for fermions. We found a rich phase structure as a function of ϕ , the fermion mass m , and the compactification size L .

In Section 2.1, we examined the phase diagram at small L by using one-loop perturbation theory for SU(2) and SU(3) gauge theories. We have shown that there is a critical boundary condition ϕ_c such that for $\phi_c < \phi < \pi$ the center symmetry is spontaneously broken for all $0 \leq mL \leq \infty$.

We also studied the dynamics of BPS and KK monopoles associated with the gauge symmetry breaking $SU(N) \rightarrow U(1)^{N-1}$ by using semiclassical methods based on the index theorem (appendix A) and found that, although they form molecules (*bions*) at $\phi \neq 0$, their non-perturbative contribution to the mass gap and string tension is exponentially suppressed by a factor $\sim e^{-1/g}$ as compared to $\phi = 0$, owing to the “real mass” of fermion zero modes that are exchanged between monopoles.

In Section 2.2, employing a phenomenological model incorporating the Yang-Mills scale of confinement, we illustrated how the phase diagram for center symmetry evolves

with varying ϕ and m and interpolates the known three limits: $\phi = 0$ (Hosotani-Ünsal regime), $\phi = \pi$ (finite temperature) and $m = \infty$ (pure Yang-Mills).

In Section 3, we adopted the PNJL model to investigate the center and chiral phase structure as a function of L and ϕ , in the chiral limit ($m = 0$). We first performed a high-temperature expansion to grasp qualitative features of the phase diagram and showed that the background Polyakov loop strongly affects chiral symmetry realization at $\phi \neq 0$. Then we numerically solved the PNJL model. The result exhibits a rich phase structure, containing all four phases (with/without chiral/center symmetry breaking) which are separated by first- and second-order phase transition lines.

One of the motivations of this work was to check the adiabatic continuity of center symmetry at $\phi = 0$, posited in Refs. [76–79]. To address this issue, we adopted two parameter sets for the PNJL model and compared the resulting phase diagrams. For the first set, the $U(1)^{N-1}$ confining phase at small L is separated from the non-Abelian confining phase at large L by a deconfined phase at intermediate L . For the second set, these two confining phases are continuously connected in the plane spanned by L and ϕ , especially on the $\phi = 0$ axis. We find that which possibility is realized is determined by the magnitude of the constituent fermion mass: if it exceeds the confining scale of the Yang-Mills theory, they are separated, and if it is smaller, they get connected.²⁹ Moreover, we also found that if the deconfined phase appears at intermediate L on the $\phi = 0$ axis, then it does not shrink but rather *expands* at $\phi \neq 0$. This means that considering QCD(adj) in a two-dimensional L - ϕ plane does not help us rescue the adiabatic continuity, if it were not present at $\phi = 0$.

We hasten to add that, even if continuity did not exist between the two confining phases, it is not detrimental at all to the confinement mechanism via bion condensation and the resurgence framework for QCD(adj) at weak coupling [76–79]. It however challenges the viewpoint that the elusive infrared renormalons on \mathbb{R}^4 may be continuously related to semiclassical configurations (bions, bion–anti-bion molecules, etc.) on $\mathbb{R}^3 \times S^1$ with small S^1 .³⁰ This is certainly an important problem and deserves further investigation.

In the PNJL model, we have used a mean-field approximation to compute the expectation values of the Polyakov loop and the chiral condensate. This is expected to be reliable at least for weak coupling $L\Lambda_{\text{QCD}} \ll 1$ where the fluctuations of the order parameters are suppressed. It is also worth mentioning that a chiral model analysis with the mean-field approximation [80] yields a phase diagram for QCD(adj) at $\phi = 0$ which is in qualitative agreement with the lattice result for the entire L range [37]. Thus it seems reasonable to expect that the present work is also providing a qualitatively correct result for QCD(adj), even though it is not theoretically warranted. As a future direction, we can employ a more refined scheme such as the Weiss mean-field approximation [11] and the functional

²⁹A similar conclusion was reached in Ref. [80] within the PNJL model at $\phi = 0$.

³⁰It should be noted that adiabatic continuity from small to large L in QCD(adj) with $N_f^W = 1$ and 5 stands on a solid ground; it is supersymmetry for $N_f^W = 1$ and infrared conformality for $N_f^W = 5$ [48] that ensures the absence of symmetry-changing phase transitions. However these are rather special theories and do not resemble QCD in the real world. The true problem posed here is whether continuity can hold in theories with continuous chiral symmetry breaking.

renormalization group [135] to check the phase diagram obtained in this work.

It would be interesting to extend our non-perturbative analysis of the $N_c = 2$ phase diagram to $N_c \geq 3$ and to the large- N_c limit. The latter is of particular importance in the context of large- N_c volume independence in QCD(adj) at $\phi = 0$ [81, 82]. Detailed analysis of large- N_c QCD(adj) at $\phi \neq 0$ may shed light on the nature of a novel fermionic symmetry in QCD(adj) recently claimed in Ref. [136].

Our idea and methodology may be applied to the study of phenomenological extra-dimensional models beyond the standard model. Although the five-dimensional Hosotani mechanism with general twisted boundary conditions is known [36], the phase structure in the space spanned by ϕ , m and L has not been investigated in details. Understanding of the phase diagram will help to find choices of parameters with desirable patterns of gauge symmetry breaking. By combining analytic methods and lattice simulations to study the phase structure, we will be able to gain deeper understanding of the gauge-Higgs unification and other extra-dimensional models.

Acknowledgments

The authors are grateful to E. Itou and K. Kashiwa for useful discussions and S. Benić for bringing Ref. [132] to their attention. Special thanks go to M. Ünsal for valuable comments on this work. The authors appreciate the KMI special lecture “Resurgence and trans-series in quantum theories” at Nagoya University and thank the organizer T. Kuroki. TM is supported by the Japan Society for the Promotion of Science (JSPS) Grants Number 26800147. TK was supported by the RIKEN iTHES Project and JSPS KAKENHI Grants Number 25887014.

A Index theorem with twisted boundary conditions

Here we study properties of the zero modes of the adjoint Dirac operator with a twisted boundary condition ϕ . The main tool is the Nye-Singer index theorem for the Dirac operator on $\mathbb{R}^3 \times S^1$ [86, 87] which interpolates the APS index theorem on \mathbb{R}^4 and the Callias index theorem on \mathbb{R}^3 . While it has been well known for the Dirac operator in the fundamental representation that the zero mode on a caloron with nontrivial holonomy “jumps” from one constituent monopole to another as ϕ is dialed [55], the behavior of adjoint zero modes has received less attention (but see Refs. [57, 61, 62]) and it is the purpose of this appendix to summarize their properties as a background material for Section 2.1.3 in the main text.

As argued in Ref. [105], smooth finite-action gauge fields on $\mathbb{R}^3 \times S^1$ can be classified by the topological charge, the magnetic charge, and the holonomy at spatial infinity. Let us assume that the holonomy at spatial infinity is given as

$$A_4|_\infty = \frac{1}{L} \text{diag}(q_1, q_2, \dots, q_N) \quad \text{with } q_1 < \dots < q_N \quad \text{and} \quad \sum_{k=1}^N q_k = 0, \quad (\text{A.1})$$

where L is the circumference of S^1 . In this setup, monopoles of N kinds are more fundamental topological objects than instantons, the latter being composed of the former. Now, we define the index $I_{\mathcal{R}}^{(\phi)}[n_1, \dots, n_N]$ of the Dirac operator in the representation \mathcal{R} , with a twisted boundary condition ϕ for fermions, as the number of right-handed normalizable zero modes minus the number of left-handed normalizable zero modes, in a background of n_k monopoles of the k -th kind ($k = 1, 2, \dots, N$). Here n_N denotes the number of KK monopoles. Then, according to Ref. [87], the index for periodic boundary condition ($\phi = 0$) is given by

$$I_{\text{adj}}^{(0)}[n_1, \dots, n_N] = 2Nn_N - \sum_{i,j=1}^N \left\lfloor \frac{q_i - q_j}{2\pi} \right\rfloor \{(n_i - n_{i-1}) - (n_j - n_{j-1})\}, \quad (\text{A.2})$$

with $\lfloor x \rfloor \equiv \max\{k \in \mathbb{Z} \mid k \leq x\}$ and $n_0 = n_N$ is understood. One can extend this formula to $\phi \neq 0$ by applying a constant Abelian gauge field equal to ϕ/L along S^1 . The result is

$$I_{\text{adj}}^{(\phi)}[n_1, \dots, n_N] = 2Nn_N - \sum_{i,j=1}^N \left\lfloor \frac{q_i - q_j + \phi}{2\pi} \right\rfloor \{(n_i - n_{i-1}) - (n_j - n_{j-1})\}. \quad (\text{A.3})$$

It is apparent from this expression that $I_{\text{adj}}^{(\phi)}$ is periodic in ϕ modulo 2π . It is also noteworthy that $I_{\text{adj}}^{(\phi)}[1, 1, \dots, 1] = 2N$, i.e., the index of BPST instanton is independent of ϕ . In what follows, we will examine the behavior of (A.3) for $N = 2$ and 3.

For $N = 2$, the holonomy may be parametrized as $A_4|_{\infty} = \frac{1}{L} \text{diag}(-q, q)$ with $q > 0$. Then

$$I_{\text{adj}}^{(\phi)}[1, 0] = 2 \left(\left\lfloor \frac{2q + \phi}{2\pi} \right\rfloor - \left\lfloor \frac{-2q + \phi}{2\pi} \right\rfloor \right), \quad (\text{A.4})$$

$$I_{\text{adj}}^{(\phi)}[0, 1] = 4 - I_{\text{adj}}^{(\phi)}[1, 0]. \quad (\text{A.5})$$

The contour plot of $I_{\text{adj}}^{(\phi)}[1, 0]$ is shown in Figure 14 (left). One can see that the index of a monopole indeed depends on the boundary condition. At $q = \pi/4$, for instance, the BPS monopole has two zero modes for $0 \leq \frac{\phi}{2\pi} < 0.25$ as shown in the figure. When $\frac{\phi}{2\pi}$ exceeds 0.25, they suddenly “jump” from the BPS monopole to the KK monopole. For $0.25 < \frac{\phi}{2\pi} < 0.75$ the KK monopole acquires all the four zero modes whereas the BPS monopole has none. Finally, when $\frac{\phi}{2\pi}$ exceeds 0.75, two of the zero modes “come back” to the BPS monopole.

Also intriguing is the fact that the index does not change with ϕ when $q = \pi/2$, which corresponds to the center-symmetric background. This particular holonomy ensures that every monopole has two zero modes for all values of ϕ . This finding is relevant to the semiclassical analysis on small S^1 in Section 2.1.3.

For $N = 3$, for simplicity of exposition, we assume a specific holonomy $A_4|_{\infty} = \frac{1}{L} \text{diag}(-q, 0, q)$ with $q > 0$. With a bit of algebra, one finds

$$I_{\text{adj}}^{(\phi)}[1, 0, 0] = I_{\text{adj}}^{(\phi)}[0, 1, 0] = \left\lfloor \frac{q + \phi}{2\pi} \right\rfloor - \left\lfloor \frac{-q + \phi}{2\pi} \right\rfloor + \left\lfloor \frac{2q + \phi}{2\pi} \right\rfloor - \left\lfloor \frac{-2q + \phi}{2\pi} \right\rfloor, \quad (\text{A.6})$$

$$I_{\text{adj}}^{(\phi)}[0, 0, 1] = 6 - 2I_{\text{adj}}^{(\phi)}[1, 0, 0]. \quad (\text{A.7})$$

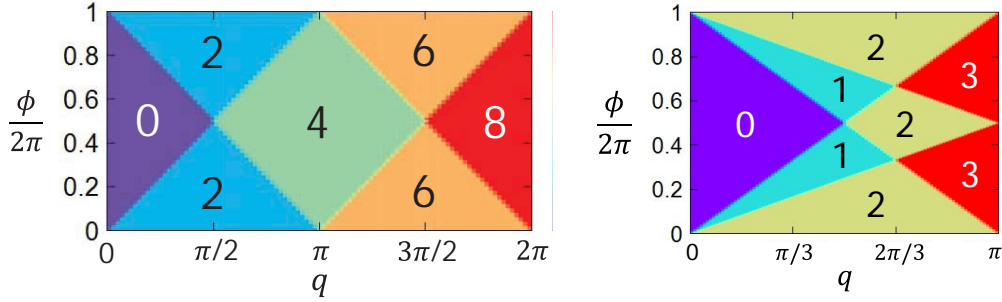


Figure 14. Index of the adjoint Dirac operator in a monopole background: $I_{\text{adj}}^{(\phi)}[1, 0]$ for $N = 2$ (left) and $I_{\text{adj}}^{(\phi)}[1, 0, 0]$ for $N = 3$ (right).

The contour plot of $I_{\text{adj}}^{(\phi)}[1, 0, 0]$ is shown in Figure 14 (right). Again one observes a nontrivial dependence of the index on ϕ , but for $q = 2\pi/3$ corresponding to the center-symmetric holonomy, the index is independent of ϕ and every monopole has two zero modes. We believe that this is true for general N : the index of every monopole should be equal to 2 for all ϕ in the center-symmetric holonomy

$$A_4|_{\infty} = \frac{1}{L} \text{diag} \left(\left(-1 + \frac{1}{N} \right) \pi, \left(-1 + \frac{3}{N} \right) \pi, \dots, \left(1 - \frac{1}{N} \right) \pi \right). \quad (\text{A.8})$$

We have numerically verified this proposition for all $N \leq 10$ using (A.3).

The behavior of anti-periodic zero modes ($\phi = \pi$) as a function of q has already been analyzed in Refs. [61, 62] on the basis of exact formulas for zero-mode densities. Their findings for $N = 2$ and 3 are totally consistent with Figure 14.

B A remark on the literature

There are a number of preceding works based on chiral effective models for QCD and QCD-like theories. In this appendix we provide a summary of literature pertinent to the present work: specifically, in Table 1 we list up papers on chiral models that either involve adjoint fermions or impose twisted boundary conditions on fermions along S^1 (or, equivalently, involve imaginary chemical potential). Our work is also listed on the bottom row. The meaning of abbreviations is as follows.

ABC: anti-periodic boundary condition, PBC: periodic boundary condition, FTBC: flavor-dependent twisted boundary condition, GN₂: the Gross-Neveu model in 2 dimensions, \mathcal{V}_g : the gluonic effective potential, NJL⁺: the NJL model with the enlarged $\text{SU}(2N_f^D)$ symmetry of adjoint fermions.

In the “large S^1 ” (“small S^1 ”) column, \bigcirc is given if \mathcal{V}_g used in each work yields the confining phase at large S^1 (the perturbative one-loop potential for Polyakov-loop eigenvalues at small S^1), respectively. Otherwise \times is given.

As is shown in the table, our work in this paper is the first study to consider generic twisted boundary conditions for adjoint fermions. We have used a four-fermi interaction

	Boundary condition	Number of colors	Chiral interaction	Rep. of quarks		Behavior of \mathcal{V}_g	
				fund.	adjoint	large S^1	small S^1
Karbstein & Thies [29]	general	—	GN ₂	—	—	—	—
Sakai et al. [30, 31]	general	3	NJL	✓	—	○	×
Kashiwa et al. [137]	general	3	NJL	✓	—	○	×
Nishimura & Ogilvie [80]	ABC/PBC	3	NJL	✓	✓	○	○
Mukherjee et al. [138]	general	—	NJL	—	—	—	—
Zhang et al. [11]	ABC	2 and 3	NJL ⁺	—	✓	○	×
Kashiwa & Misumi [112]	ABC/PBC	3	NJL	✓	✓	×	○
Kouno et al. [134]	ABC/PBC/ FTBC	3	NJL	✓	✓	○ (ABC/PBC) × (FTBC)	× (ABC/PBC) ○ (FTBC)
Benić [132]	general	—	NJL	—	—	—	—
This work	general	2	NJL ⁺	—	✓	○	○

Table 1. Chiral effective models with unorthodox fermionic boundary conditions (in chronological order). See the main text for the definition of abbreviations.

derived in Ref. [11] to reflect the correct flavor symmetry of adjoint fermions. Another important ingredient of our model is the use of a gluonic potential \mathcal{V}_g proposed in Ref. [80] which can produce a confining phase at large S^1 and a perturbative one-loop potential (2.6) at small S^1 . This property is essential for us to be able to describe the gauge-symmetry-broken phase at small S^1 and the confining phase at large S^1 in a unified manner.

References

- [1] J. B. Kogut, J. Polonyi, H. Wyld, and D. Sinclair, *Hierarchical Mass Scales in Lattice Gauge Theories With Dynamical Light Fermions*, *Phys.Rev.Lett.* **54** (1985) 1980.
- [2] J. B. Kogut, *SIMULATING SIMPLE SUPERSYMMETRIC FIELD THEORIES*, *Phys.Lett.* **B187** (1987) 347.
- [3] F. Karsch and M. Lutgemeier, *Deconfinement and chiral symmetry restoration in an $SU(3)$ gauge theory with adjoint fermions*, *Nucl.Phys.* **B550** (1999) 449–464, [[hep-lat/9812023](#)].
- [4] J. Engels, S. Holtmann, and T. Schulze, *Scaling and Goldstone effects in a QCD with two flavors of adjoint quarks*, *Nucl.Phys.* **B724** (2005) 357–379, [[hep-lat/0505008](#)].
- [5] M. G. Alford, A. Kapustin, and F. Wilczek, *Imaginary chemical potential and finite fermion density on the lattice*, *Phys. Rev.* **D59** (1999) 054502, [[hep-lat/9807039](#)].
- [6] J. B. Kogut, M. A. Stephanov, D. Toublan, J. J. M. Verbaarschot, and A. Zhitnitsky, *QCD-like theories at finite baryon density*, *Nucl. Phys.* **B582** (2000) 477–513, [[hep-ph/0001171](#)].
- [7] S. Hands et al., *Numerical study of dense adjoint matter in two color QCD*, *Eur. Phys. J.* **C17** (2000) 285–302, [[hep-lat/0006018](#)].
- [8] H. Leutwyler and A. V. Smilga, *Spectrum of Dirac operator and role of winding number in QCD*, *Phys. Rev.* **D46** (1992) 5607–5632.

- [9] K. Splittorff, D. T. Son, and M. A. Stephanov, *QCD-like Theories at Finite Baryon and Isospin Density*, *Phys. Rev.* **D64** (2001) 016003, [[hep-ph/0012274](#)].
- [10] T. Kanazawa, T. Wettig, and N. Yamamoto, *Singular values of the Dirac operator in dense QCD-like theories*, *JHEP* **12** (2011) 007, [[arXiv:1110.5858](#)].
- [11] T. Zhang, T. Brauner, and D. H. Rischke, *QCD-like theories at nonzero temperature and density*, *JHEP* **06** (2010) 064, [[arXiv:1005.2928](#)].
- [12] J. Braun and T. K. Herbst, *On the Relation of the Deconfinement and the Chiral Phase Transition in Gauge Theories with Fundamental and Adjoint Matter*, [arXiv:1205.0779](#).
- [13] L. He, S. Mao, and P. Zhuang, *BCS-BEC crossover in relativistic Fermi systems*, *Int.J.Mod.Phys.* **A28** (2013) 1330054, [[arXiv:1311.6704](#)].
- [14] E. Witten, *Constraints on Supersymmetry Breaking*, *Nucl. Phys.* **B202** (1982) 253.
- [15] B. Lucini and M. Panero, *SU(N) gauge theories at large N*, *Phys.Rept.* **526** (2013) 93–163, [[arXiv:1210.4997](#)].
- [16] C. T. Hill and E. H. Simmons, *Strong dynamics and electroweak symmetry breaking*, *Phys.Rept.* **381** (2003) 235–402, [[hep-ph/0203079](#)].
- [17] M. Shifman, *Remarks on Adjoint QCD with k Flavors, $k \geq 2$* , *Mod.Phys.Lett.* **A28** (2013) 1350179, [[arXiv:1307.5826](#)].
- [18] N. Seiberg and E. Witten, *Gauge dynamics and compactification to three-dimensions*, [hep-th/9607163](#).
- [19] N. M. Davies, T. J. Hollowood, V. V. Khoze, and M. P. Mattis, *Gluino condensate and magnetic monopoles in supersymmetric gluodynamics*, *Nucl.Phys.* **B559** (1999) 123–142, [[hep-th/9905015](#)].
- [20] N. M. Davies, T. J. Hollowood, and V. V. Khoze, *Monopoles, affine algebras and the gluino condensate*, *J.Math.Phys.* **44** (2003) 3640–3656, [[hep-th/0006011](#)].
- [21] E. Poppitz, T. Schafer, and M. Unsal, *Continuity, Deconfinement, and (Super) Yang-Mills Theory*, *JHEP* **1210** (2012) 115, [[arXiv:1205.0290](#)].
- [22] A. Roberge and N. Weiss, *Gauge Theories With Imaginary Chemical Potential and the Phases of QCD*, *Nucl.Phys.* **B275** (1986) 734.
- [23] P. de Forcrand and O. Philipsen, *The QCD phase diagram for small densities from imaginary chemical potential*, *Nucl.Phys.* **B642** (2002) 290–306, [[hep-lat/0205016](#)].
- [24] M. D’Elia and M.-P. Lombardo, *Finite density QCD via imaginary chemical potential*, *Phys.Rev.* **D67** (2003) 014505, [[hep-lat/0209146](#)].
- [25] M. D’Elia and M. P. Lombardo, *QCD thermodynamics from an imaginary $\mu(B)$: Results on the four flavor lattice model*, *Phys.Rev.* **D70** (2004) 074509, [[hep-lat/0406012](#)].
- [26] H.-S. Chen and X.-Q. Luo, *Phase diagram of QCD at finite temperature and chemical potential from lattice simulations with dynamical Wilson quarks*, *Phys.Rev.* **D72** (2005) 034504, [[hep-lat/0411023](#)].
- [27] P. de Forcrand and O. Philipsen, *Constraining the QCD phase diagram by tricritical lines at imaginary chemical potential*, *Phys.Rev.Lett.* **105** (2010) 152001, [[arXiv:1004.3144](#)].
- [28] G. Aarts, *Complex Langevin dynamics and other approaches at finite chemical potential*, *PoS LATTICE2012* (2012) 017, [[arXiv:1302.3028](#)].

- [29] F. Karbstein and M. Thies, *How to get from imaginary to real chemical potential*, *Phys.Rev.* **D75** (2007) 025003, [[hep-th/0610243](#)].
- [30] Y. Sakai, K. Kashiwa, H. Kouno, and M. Yahiro, *Polyakov loop extended NJL model with imaginary chemical potential*, *Phys.Rev.* **D77** (2008) 051901, [[arXiv:0801.0034](#)].
- [31] Y. Sakai, K. Kashiwa, H. Kouno, and M. Yahiro, *Phase diagram in the imaginary chemical potential region and extended $Z(3)$ symmetry*, *Phys.Rev.* **D78** (2008) 036001, [[arXiv:0803.1902](#)].
- [32] C. Gattringer, *Linking confinement to spectral properties of the Dirac operator*, *Phys.Rev.Lett.* **97** (2006) 032003, [[hep-lat/0605018](#)].
- [33] E. Bilgici, F. Bruckmann, C. Gattringer, and C. Hagen, *Dual quark condensate and dressed Polyakov loops*, *Phys.Rev.* **D77** (2008) 094007, [[arXiv:0801.4051](#)].
- [34] E. Bilgici, C. Gattringer, E.-M. Ilgenfritz, and A. Maas, *Adjoint quarks and fermionic boundary conditions*, *JHEP* **0911** (2009) 035, [[arXiv:0904.3450](#)].
- [35] E. Bilgici, F. Bruckmann, J. Danzer, C. Gattringer, C. Hagen, et al., *Fermionic boundary conditions and the finite temperature transition of QCD*, *Few Body Syst.* **47** (2010) 125–135, [[arXiv:0906.3957](#)].
- [36] Y. Hosotani, *Dynamics of Nonintegrable Phases and Gauge Symmetry Breaking*, *Annals Phys.* **190** (1989) 233.
- [37] G. Cossu and M. D’Elia, *Finite size phase transitions in QCD with adjoint fermions*, *JHEP* **0907** (2009) 048, [[arXiv:0904.1353](#)].
- [38] G. Cossu, H. Hatanaka, Y. Hosotani, and J.-I. Noaki, *Polyakov loops and the Hosotani mechanism on the lattice*, [arXiv:1309.4198](#).
- [39] N. Manton, *A New Six-Dimensional Approach to the Weinberg-Salam Model*, *Nucl.Phys.* **B158** (1979) 141.
- [40] D. Fairlie, *Higgs’ Fields and the Determination of the Weinberg Angle*, *Phys.Lett.* **B82** (1979) 97.
- [41] D. Fairlie, *Two Consistent Calculations of the Weinberg Angle*, *J.Phys.* **G5** (1979) L55.
- [42] Y. Hosotani, *Dynamical Mass Generation by Compact Extra Dimensions*, *Phys.Lett.* **B126** (1983) 309.
- [43] M. Unsal, *Abelian duality, confinement, and chiral symmetry breaking in QCD(adj)*, *Phys.Rev.Lett.* **100** (2008) 032005, [[arXiv:0708.1772](#)].
- [44] M. Unsal, *Magnetic bion condensation: A New mechanism of confinement and mass gap in four dimensions*, *Phys.Rev.* **D80** (2009) 065001, [[arXiv:0709.3269](#)].
- [45] A. M. Polyakov, *Quark Confinement and Topology of Gauge Groups*, *Nucl.Phys.* **B120** (1977) 429–458.
- [46] N. Seiberg and E. Witten, *Electric - magnetic duality, monopole condensation, and confinement in $N=2$ supersymmetric Yang-Mills theory*, *Nucl.Phys.* **B426** (1994) 19–52, [[hep-th/9407087](#)].
- [47] M. Shifman and M. Unsal, *QCD-like Theories on $R(3) \times S(1)$: A Smooth Journey from Small to Large $r(S(1))$ with Double-Trace Deformations*, *Phys.Rev.* **D78** (2008) 065004, [[arXiv:0802.1232](#)].

- [48] E. Poppitz and M. Unsal, *Conformality or confinement: (IR)relevance of topological excitations*, *JHEP* **0909** (2009) 050, [[arXiv:0906.5156](#)].
- [49] E. Poppitz and T. Sulejmanpasic, *(S)QCD on $\mathbb{R}^3 \times S^1$: Screening of Polyakov loop by fundamental quarks and the demise of semi-classics*, *JHEP* **1309** (2013) 128, [[arXiv:1307.1317](#)].
- [50] K.-M. Lee and P. Yi, *Monopoles and instantons on partially compactified D-branes*, *Phys.Rev.* **D56** (1997) 3711–3717, [[hep-th/9702107](#)].
- [51] K.-M. Lee and C.-h. Lu, *$SU(2)$ calorons and magnetic monopoles*, *Phys.Rev.* **D58** (1998) 025011, [[hep-th/9802108](#)].
- [52] T. C. Kraan and P. van Baal, *Periodic instantons with nontrivial holonomy*, *Nucl.Phys.* **B533** (1998) 627–659, [[hep-th/9805168](#)].
- [53] T. C. Kraan and P. van Baal, *Monopole constituents inside $SU(n)$ calorons*, *Phys.Lett.* **B435** (1998) 389–395, [[hep-th/9806034](#)].
- [54] M. Garcia Perez, A. Gonzalez-Arroyo, C. Pena, and P. van Baal, *Weyl-Dirac zero mode for calorons*, *Phys.Rev.* **D60** (1999) 031901, [[hep-th/9905016](#)].
- [55] F. Bruckmann, D. Negradi, and P. van Baal, *Instantons and constituent monopoles*, *Acta Phys.Polon.* **B34** (2003) 5717–5750, [[hep-th/0309008](#)].
- [56] D. Diakonov, N. Gromov, V. Petrov, and S. Slizovskiy, *Quantum weights of dyons and of instantons with nontrivial holonomy*, *Phys.Rev.* **D70** (2004) 036003, [[hep-th/0404042](#)].
- [57] M. Garcia Perez and A. Gonzalez-Arroyo, *Gluino zero-modes for non-trivial holonomy calorons*, *JHEP* **0611** (2006) 091, [[hep-th/0609058](#)].
- [58] D. Diakonov and V. Petrov, *Confining ensemble of dyons*, *Phys.Rev.* **D76** (2007) 056001, [[arXiv:0704.3181](#)].
- [59] M. Unsal and L. G. Yaffe, *Center-stabilized Yang-Mills theory: Confinement and large N volume independence*, *Phys.Rev.* **D78** (2008) 065035, [[arXiv:0803.0344](#)].
- [60] D. Diakonov, *Statistical physics of dyons and confinement*, *Acta Phys.Polon.* **B39** (2008) 3365–3393, [[arXiv:0807.0902](#)].
- [61] M. Garcia Perez, A. Gonzalez-Arroyo, and A. Sastre, *Gluino zero-modes for calorons at finite temperature*, *Phys.Lett.* **B668** (2008) 340–345, [[arXiv:0807.2285](#)].
- [62] M. Garcia Perez, A. Gonzalez-Arroyo, and A. Sastre, *Adjoint fermion zero-modes for $SU(N)$ calorons*, *JHEP* **0906** (2009) 065, [[arXiv:0905.0645](#)].
- [63] P. N. Meisinger and M. C. Ogilvie, *String Tension Scaling in High-Temperature Confined $SU(N)$ Gauge Theories*, *Phys.Rev.* **D81** (2010) 025012, [[arXiv:0905.3577](#)].
- [64] D. Diakonov, *Topology and confinement*, *Nucl.Phys.Proc.Suppl.* **195** (2009) 5–45, [[arXiv:0906.2456](#)].
- [65] D. Diakonov and V. Petrov, *Confinement and deconfinement for any gauge group from dyons viewpoint*, *AIP Conf.Proc.* **1343** (2011) 69–74, [[arXiv:1011.5636](#)].
- [66] M. M. Anber and E. Poppitz, *Microscopic Structure of Magnetic Bions*, *JHEP* **1106** (2011) 136, [[arXiv:1105.0940](#)].
- [67] M. C. Ogilvie, *Phases of Gauge Theories*, *J.Phys.* **A45** (2012) 483001, [[arXiv:1211.2843](#)].

- [68] P. F. Bedaque, *Aharonov-Bohm effect and nucleon nucleon phase shifts on the lattice*, *Phys.Lett.* **B593** (2004) 82–88, [[nucl-th/0402051](#)].
- [69] T. Mehen and B. C. Tiburzi, *Quarks with twisted boundary conditions in the epsilon regime*, *Phys.Rev.* **D72** (2005) 014501, [[hep-lat/0505014](#)].
- [70] P. H. Damgaard, U. M. Heller, K. Splittorff, and B. Svetitsky, *A new method for determining $F(\pi)$ on the lattice*, *Phys. Rev.* **D72** (2005) 091501, [[hep-lat/0508029](#)].
- [71] P. H. Damgaard, U. M. Heller, K. Splittorff, B. Svetitsky, and D. Toublan, *Extracting $F(\pi)$ from small lattices: Unquenched results*, *Phys. Rev.* **D73** (2006) 074023, [[hep-lat/0602030](#)].
- [72] T. DeGrand and R. Hoffmann, *QCD with one compact spatial dimension*, *JHEP* **0702** (2007) 022, [[hep-lat/0612012](#)].
- [73] S. Ozaki and S. Sasaki, *Lüscher’s finite size method with twisted boundary conditions: an application to J/ψ - ϕ system to search for narrow resonance*, *Phys.Rev.* **D87** (2013) 014506, [[arXiv:1211.5512](#)].
- [74] J. C. Myers and M. C. Ogilvie, *Phase diagrams of $SU(N)$ gauge theories with fermions in various representations*, *JHEP* **0907** (2009) 095, [[arXiv:0903.4638](#)].
- [75] E. Shuryak, *Physics of Strongly coupled Quark-Gluon Plasma*, *Prog.Part.Nucl.Phys.* **62** (2009) 48–101, [[arXiv:0807.3033](#)].
- [76] P. Argyres and M. Unsal, *A semiclassical realization of infrared renormalons*, *Phys.Rev.Lett.* **109** (2012) 121601, [[arXiv:1204.1661](#)].
- [77] P. C. Argyres and M. Unsal, *The semi-classical expansion and resurgence in gauge theories: new perturbative, instanton, bion, and renormalon effects*, *JHEP* **1208** (2012) 063, [[arXiv:1206.1890](#)].
- [78] G. V. Dunne and M. Unsal, *Resurgence and Trans-series in Quantum Field Theory: The $CP(N-1)$ Model*, *JHEP* **1211** (2012) 170, [[arXiv:1210.2423](#)].
- [79] G. V. Dunne and M. Unsal, *Continuity and Resurgence: towards a continuum definition of the $CP(N-1)$ model*, *Phys.Rev.* **D87** (2013) 025015, [[arXiv:1210.3646](#)].
- [80] H. Nishimura and M. C. Ogilvie, *A PNJL Model for Adjoint Fermions with Periodic Boundary Conditions*, *Phys.Rev.* **D81** (2010) 014018, [[arXiv:0911.2696](#)].
- [81] P. Kovtun, M. Unsal, and L. G. Yaffe, *Volume independence in large $N(c)$ QCD-like gauge theories*, *JHEP* **0706** (2007) 019, [[hep-th/0702021](#)].
- [82] M. Unsal and L. G. Yaffe, *Large- N volume independence in conformal and confining gauge theories*, *JHEP* **1008** (2010) 030, [[arXiv:1006.2101](#)].
- [83] P. N. Meisinger and M. C. Ogilvie, *Chiral symmetry restoration and $Z(N)$ symmetry*, *Phys.Lett.* **B379** (1996) 163–168, [[hep-lat/9512011](#)].
- [84] K. Fukushima, *Chiral effective model with the Polyakov loop*, *Phys. Lett.* **B591** (2004) 277–284, [[hep-ph/0310121](#)].
- [85] C. Ratti, M. A. Thaler, and W. Weise, *Phases of QCD: Lattice thermodynamics and a field theoretical model*, *Phys.Rev.* **D73** (2006) 014019, [[hep-ph/0506234](#)].
- [86] T. M. Nye and M. A. Singer, *An L^{**2} index theorem for Dirac operators on $S^{**1} \times R^{**3}$* , *J.Funct.Anal.* (2000) [[math/0009144](#)].

- [87] E. Poppitz and M. Unsal, *Index theorem for topological excitations on $R^{*3} \times S^{*1}$ and Chern-Simons theory*, *JHEP* **0903** (2009) 027, [[arXiv:0812.2085](#)].
- [88] M. E. Peskin and D. V. Schroeder, *An Introduction to quantum field theory*, . Reading, USA: Addison-Wesley (1995) 842 p.
- [89] A. Redlich and L. Wijewardhana, *Induced Chern-simons Terms at High Temperatures and Finite Densities*, *Phys.Rev.Lett.* **54** (1985) 970.
- [90] A. Niemi and G. Semenoff, *A Comment on ‘Induced Chern-simons Terms at High Temperatures and Finite Densities’*, *Phys.Rev.Lett.* **54** (1985) 2166.
- [91] S. Catterall, J. Giedt, F. Sannino, and J. Schneible, *Phase diagram of $SU(2)$ with 2 flavors of dynamical adjoint quarks*, *JHEP* **0811** (2008) 009, [[arXiv:0807.0792](#)].
- [92] A. J. Hietanen, J. Rantaharju, K. Rummukainen, and K. Tuominen, *Spectrum of $SU(2)$ lattice gauge theory with two adjoint Dirac flavours*, *JHEP* **0905** (2009) 025, [[arXiv:0812.1467](#)].
- [93] A. J. Hietanen, K. Rummukainen, and K. Tuominen, *Evolution of the coupling constant in $SU(2)$ lattice gauge theory with two adjoint fermions*, *Phys.Rev.* **D80** (2009) 094504, [[arXiv:0904.0864](#)].
- [94] L. Del Debbio, B. Lucini, A. Patella, C. Pica, and A. Rago, *Conformal versus confining scenario in $SU(2)$ with adjoint fermions*, *Phys.Rev.* **D80** (2009) 074507, [[arXiv:0907.3896](#)].
- [95] T. DeGrand, Y. Shamir, and B. Svetitsky, *Infrared fixed point in $SU(2)$ gauge theory with adjoint fermions*, *Phys.Rev.* **D83** (2011) 074507, [[arXiv:1102.2843](#)].
- [96] A. Athenodorou, E. Bennett, G. Bergner, B. Lucini, and A. Patella, *First results for $SU(2)$ Yang-Mills with one adjoint Dirac Fermion*, *PoS LATTICE 2013* (2013) 066, [[arXiv:1311.4155](#)].
- [97] T. DeGrand, Y. Shamir, and B. Svetitsky, *Near the sill of the conformal window: gauge theories with fermions in two-index representations*, *Phys.Rev.* **D88** (2013) 054505, [[arXiv:1307.2425](#)].
- [98] T. DeGrand, Y. Shamir, and B. Svetitsky, *Gauge theories with fermions in two-index representations*, [arXiv:1310.2128](#).
- [99] T. Azeyanagi, M. Hanada, M. Unsal, and R. Yacoby, *Large- N reduction in QCD-like theories with massive adjoint fermions*, *Phys.Rev.* **D82** (2010) 125013, [[arXiv:1006.0717](#)].
- [100] S. Catterall, R. Galvez, and M. Unsal, *Realization of Center Symmetry in Two Adjoint Flavor Large- N Yang-Mills*, *JHEP* **1008** (2010) 010, [[arXiv:1006.2469](#)].
- [101] B. Bringoltz, M. Koren, and S. R. Sharpe, *Large- N reduction in QCD with two adjoint Dirac fermions*, *Phys.Rev.* **D85** (2012) 094504, [[arXiv:1106.5538](#)].
- [102] A. Gonzalez-Arroyo and M. Okawa, *Twisted reduction in large N QCD with two adjoint Wilson fermions*, *PoS LATTICE2012* (2012) 046, [[arXiv:1210.7881](#)].
- [103] A. Gonzalez-Arroyo and M. Okawa, *Twisted space-time reduced model of large N QCD with two adjoint Wilson fermions*, *Phys.Rev.* **D88** (2013) 014514, [[arXiv:1305.6253](#)].
- [104] A. Gonzalez-Arroyo and M. Okawa, *Twisted reduction in large N QCD with adjoint Wilson fermions*, [arXiv:1311.3778](#).
- [105] D. J. Gross, R. D. Pisarski, and L. G. Yaffe, *QCD and Instantons at Finite Temperature*, *Rev.Mod.Phys.* **53** (1981) 43.

- [106] N. Weiss, *The Effective Potential for the Order Parameter of Gauge Theories at Finite Temperature*, *Phys.Rev.* **D24** (1981) 475.
- [107] J. C. Myers and M. C. Ogilvie, *New phases of $SU(3)$ and $SU(4)$ at finite temperature*, *Phys.Rev.* **D77** (2008) 125030, [[arXiv:0707.1869](#)].
- [108] M. Shifman and M. Unsal, *Multiflavor QCD* on $R(3) \times S(1)$: Studying Transition From Abelian to Non-Abelian Confinement*, *Phys.Lett.* **B681** (2009) 491–494, [[arXiv:0901.3743](#)].
- [109] T. W. Kirkman and C. K. Zachos, *Asymptotic Analysis of the Monopole Structure*, *Phys.Rev.* **D24** (1981) 999.
- [110] V. V. Khoze and A. Yung, *Instanton vacuum in thermal QCD*, *Z.Phys.* **C50** (1991) 155–164.
- [111] T. Schafer, E. V. Shuryak, and J. Verbaarschot, *The Chiral phase transition and instanton - anti-instanton molecules*, *Phys.Rev.* **D51** (1995) 1267–1281, [[hep-ph/9406210](#)].
- [112] K. Kashiwa and T. Misumi, *Phase structure and Hosotani mechanism in gauge theories with compact dimensions revisited*, *JHEP* **1305** (2013) 042, [[arXiv:1302.2196](#)].
- [113] P. N. Meisinger, T. R. Miller, and M. C. Ogilvie, *Phenomenological equations of state for the quark gluon plasma*, *Phys.Rev.* **D65** (2002) 034009, [[hep-ph/0108009](#)].
- [114] M. Ogilvie, *Confinement in high-temperature lattice gauge theories*, *PoS LATTICE2012* (2012) 085, [[arXiv:1211.1358](#)].
- [115] H. Abuki and K. Fukushima, *Gauge dynamics in the PNJL model: Color neutrality and Casimir scaling*, *Phys.Lett.* **B676** (2009) 57–62, [[arXiv:0901.4821](#)].
- [116] S. Gupta, K. Huebner, and O. Kaczmarek, *Renormalized Polyakov loops in many representations*, *Phys.Rev.* **D77** (2008) 034503, [[arXiv:0711.2251](#)].
- [117] C. Sasaki and K. Redlich, *An Effective gluon potential and hybrid approach to Yang-Mills thermodynamics*, *Phys.Rev.* **D86** (2012) 014007, [[arXiv:1204.4330](#)].
- [118] M. Ruggieri, P. Alba, P. Castorina, S. Plumari, C. Ratti, et al., *Polyakov Loop and Gluon Quasiparticles in Yang-Mills Thermodynamics*, *Phys.Rev.* **D86** (2012) 054007, [[arXiv:1204.5995](#)].
- [119] M. Creutz, *The 't Hooft vertex revisited*, *Annals Phys.* **323** (2008) 2349–2365, [[arXiv:0711.2640](#)].
- [120] M. Unsal, *Quantum phase transitions and new scales in QCD-like theories*, *Phys.Rev.Lett.* **102** (2009) 182002, [[arXiv:0807.0466](#)].
- [121] F. Basile, A. Pelissetto, and E. Vicari, *The Finite-temperature chiral transition in QCD with adjoint fermions*, *JHEP* **0502** (2005) 044, [[hep-th/0412026](#)].
- [122] F. Basile, A. Pelissetto, and E. Vicari, *Finite-temperature chiral transition in QCD with quarks in the fundamental and adjoint representation*, *PoS LAT2005* (2006) 199, [[hep-lat/0509018](#)].
- [123] G. Bergner, P. Giudice, G. Mnster, S. Piemonte, and D. Sandbrink, *Phase structure of the $N=1$ supersymmetric Yang-Mills theory at finite temperature*, [arXiv:1405.3180](#).
- [124] C. Vafa and E. Witten, *Restrictions on Symmetry Breaking in Vector-Like Gauge Theories*, *Nucl. Phys.* **B234** (1984) 173.
- [125] D. Weingarten, *Mass Inequalities for QCD*, *Phys. Rev. Lett.* **51** (1983) 1830.

- [126] E. Witten, *Some Inequalities Among Hadron Masses*, *Phys. Rev. Lett.* **51** (1983) 2351.
- [127] S. Nussinov, *MASS INEQUALITIES IN QCD*, *Phys. Rev. Lett.* **52** (1984) 966.
- [128] R. D. Pisarski and F. Wilczek, *Remarks on the Chiral Phase Transition in Chromodynamics*, *Phys.Rev.* **D29** (1984) 338–341.
- [129] S. P. Klevansky, *The Nambu-Jona-Lasinio model of quantum chromodynamics*, *Rev. Mod. Phys.* **64** (1992) 649–708.
- [130] T. Hatsuda and T. Kunihiro, *QCD phenomenology based on a chiral effective Lagrangian*, *Phys. Rept.* **247** (1994) 221–367, [[hep-ph/9401310](#)].
- [131] B. Klajn, *Exact high temperature expansion of the one-loop thermodynamic potential with complex chemical potential*, *Phys.Rev.* **D89** (2014) 036001, [[arXiv:1311.2512](#)].
- [132] S. Benić, *Physical interpretation of the dressed Polyakov loop in the Nambu-Jona-Lasinio model*, *Phys.Rev.* **D88** (2013) 077501, [[arXiv:1305.6567](#)].
- [133] J. Braun, J.-W. Chen, J. Deng, J. E. Drut, B. Friman, et al., *A glance at the imaginary world of ultracold atoms*, *Phys.Rev.Lett.* **110** (2013) 130404, [[arXiv:1209.3319](#)].
- [134] H. Kouno, T. Misumi, K. Kashiwa, T. Makiyama, T. Sasaki, et al., *Differences and similarities between fundamental and adjoint matters in $SU(N)$ gauge theories*, *Phys.Rev.* **D88** (2013) 016002, [[arXiv:1304.3274](#)].
- [135] J. Berges, N. Tetradis, and C. Wetterich, *Nonperturbative renormalization flow in quantum field theory and statistical physics*, *Phys.Rept.* **363** (2002) 223–386, [[hep-ph/0005122](#)].
- [136] G. Basar, A. Cherman, D. Dorigoni, and M. Unsal, *Large N Volume Independence and an Emergent Fermionic Symmetry*, *Phys. Rev. Lett.* **111**, **121601** (2013) 121601, [[arXiv:1306.2960](#)].
- [137] K. Kashiwa, H. Kouno, and M. Yahiro, *Dual quark condensate in the Polyakov-loop extended NJL model*, *Phys.Rev.* **D80** (2009) 117901, [[arXiv:0908.1213](#)].
- [138] T. K. Mukherjee, H. Chen, and M. Huang, *Chiral condensate and dressed Polyakov loop in the Nambu-Jona-Lasinio model*, *Phys.Rev.* **D82** (2010) 034015, [[arXiv:1005.2482](#)].